



## Article

# Improving Approaches to Mapping Seagrass within the Great Barrier Reef: From Field to Spaceborne Earth Observation

Len J. McKenzie <sup>1,2,\*</sup> , Lucas A. Langlois <sup>1</sup> and Chris M. Roelfsema <sup>3</sup>

<sup>1</sup> Centre for Tropical Water and Aquatic Ecosystem Research (TropWATER), James Cook University, Cairns, QLD 4870, Australia; lucas.langlois@jcu.edu.au

<sup>2</sup> Seagrass-Watch, Cairns, QLD 4870, Australia

<sup>3</sup> Remote Sensing Research Centre, School of Earth and Environmental Sciences, The University of Queensland, Brisbane, QLD 4072, Australia; c.roelfsema@uq.edu.au

\* Correspondence: len.mckenzie@jcu.edu.au; Tel.: +61-7-4232-2012

**Abstract:** Seagrass meadows are a key ecosystem of the Great Barrier Reef World Heritage Area, providing one of the natural heritage attributes underpinning the reef's outstanding universal value. We reviewed approaches employed to date to create maps of seagrass meadows in the optically complex waters of the Great Barrier Reef and explored enhanced mapping approaches with a focus on emerging technologies, and key considerations for future mapping. Our review showed that field-based mapping of seagrass has traditionally been the most common approach in the GBRWHA, with few attempts to adopt remote sensing approaches and emerging technologies. Using a series of case studies to harness the power of machine- and deep-learning, we mapped seagrass cover with PlanetScope and UAV-captured imagery in a variety of settings. Using a machine-learning pixel-based classification coupled with a bootstrapping process, we were able to significantly improve maps of seagrass, particularly in low cover, fragmented and complex habitats. We also used deep-learning models to derive enhanced maps from UAV imagery. Combined, these lessons and emerging technologies show that more accurate and efficient seagrass mapping approaches are possible, producing maps of higher confidence for users and enabling the upscaling of seagrass mapping into the future.

**Keywords:** seagrass; Great Barrier Reef; mapping; earth observing; machine-learning; deep-learning; UAV; spaceborne; map confidence



**Citation:** McKenzie, L.J.; Langlois, L.A.; Roelfsema, C.M. Improving Approaches to Mapping Seagrass within the Great Barrier Reef: From Field to Spaceborne Earth Observation. *Remote Sens.* **2022**, *14*, 2604. <https://doi.org/10.3390/rs14112604>

Academic Editors: Kadija Oubelkheir, Michelle Devlin and Caroline Petus

Received: 21 March 2022

Accepted: 26 May 2022

Published: 29 May 2022

**Publisher's Note:** MDPI stays neutral with regard to jurisdictional claims in published maps and institutional affiliations.



**Copyright:** © 2022 by the authors. Licensee MDPI, Basel, Switzerland. This article is an open access article distributed under the terms and conditions of the Creative Commons Attribution (CC BY) license (<https://creativecommons.org/licenses/by/4.0/>).

## 1. Introduction

Since 11 June 1770 when the Great Barrier Reef (GBR) was first recorded in western marine charts [1,2], approaches to mapping the GBR and its ecosystems have advanced significantly. The earliest record of seagrass within the GBR waters was by the British botanist Robert Brown aboard the HMS *Investigator* in the early 1800s [3,4]. However, interest in seagrass and seagrass ecosystems was marginalised in the research and assessment literature of the GBR until well into the 20th century. It was with the recognition of the importance of seagrasses to dugong (*Dugong dugon*) and fisheries that attention on the location and variety of seagrass habitats came to significance [5,6]. This also coincided with the inscribing of the Great Barrier Reef Marine Park (Figure 1) on the World Heritage List in October 1981. A key component of the listing was the importance of the region to species of conservation concern, including dugong and green turtle (*Chelonia mydas*) and their habitats, i.e., seagrass meadows. This prompted a critical need for an inventory of the seagrass meadows of the GBR within the immediate decade.

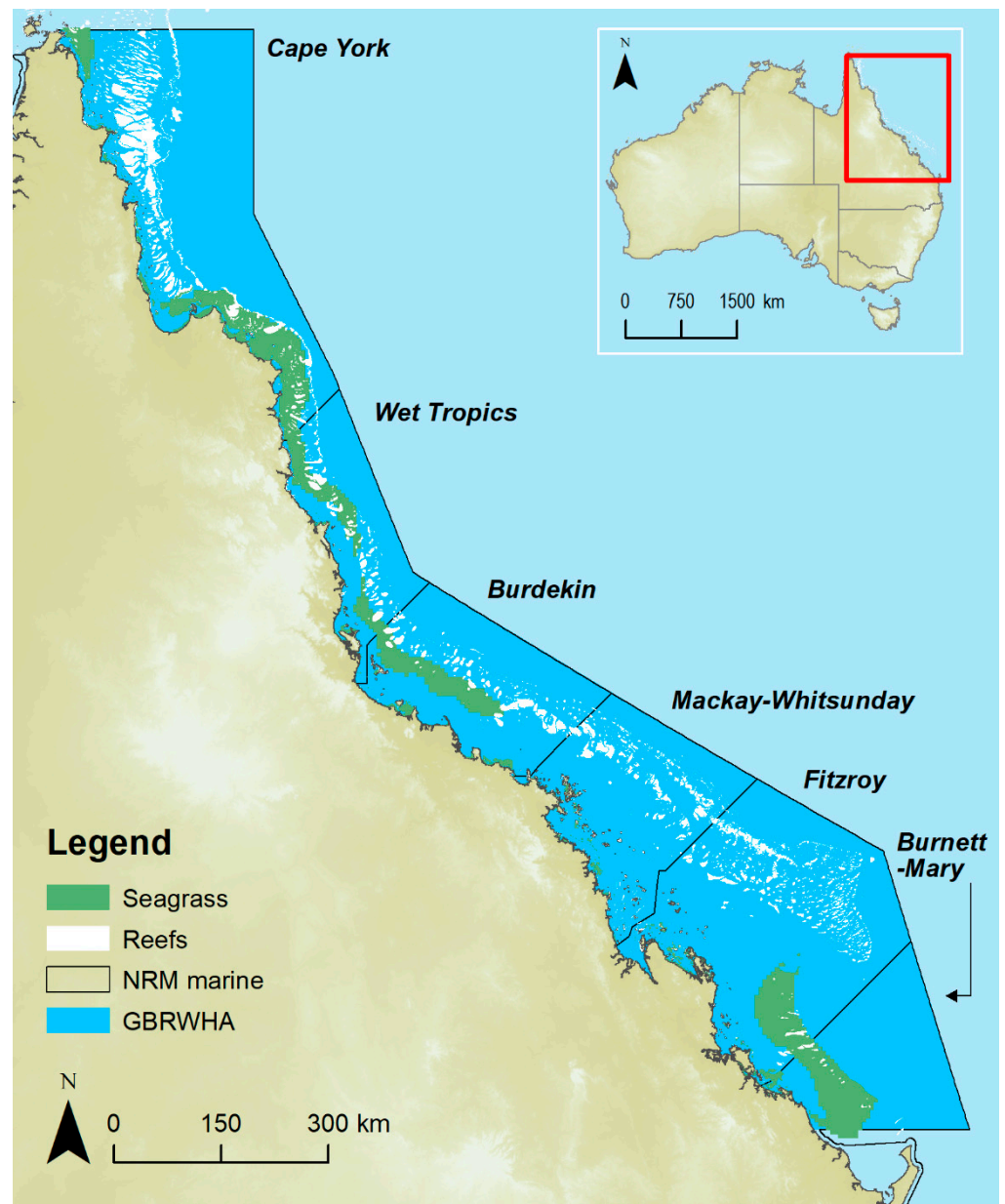


**Figure 1.** Seagrass meadows composite map [7,8], coral reefs [9], the Great Barrier Reef World Heritage Area, and marine portions of each Natural Resource Management (NRM) region.

Current estimates are that seagrass meadows cover approximately 35,679 km<sup>2</sup> of the seafloor of the GBR World Heritage Area (GBRWHA) [10] (Figure 1); which is a greater area than that covered by coral reefs. Seagrasses provide critical goods and benefits such as food for marine green turtles and dugongs, fisheries habitat, coastal protection, nutrient cycling, improving water quality, and reducing pathogenic bacteria to the benefit of humans, fishes, and marine invertebrates such as coral [11–15]. In addition, the incorporation of carbon within seagrass tissues can affect local pH, thereby helping to mitigate the effects of ocean acidification affecting coral reefs, and the retention of carbon within seagrass meadow sediments contributes significantly to climate change mitigation as well [16–18]. Therefore, the ecosystem contributions provided by seagrasses make them a high conservation priority [19,20].

In recognition of the critical importance of seagrasses, there is a pressing need to complete and/or improve maps of seagrass spatial extent for conservation and natural capital accounting. This is particularly challenging in tropical regions where seagrass

ecosystems are diverse and dynamic, varying spatially and temporally in their distribution and abundance, often with low seagrass cover, growing in a variety of complex substrates and optically complex waters [5,21]. As a consequence of the high diversity of seagrass species across a range of habitats, responses to environmental drivers in the tropics (e.g., terrigenous runoff and physical disturbance) can be highly variable across a range of temporal and spatial scales (e.g., weeks to years, metres to kilometres) [22,23].

Seagrasses within the GBRWHA have been extensively mapped over the last 30 years [10], using a variety of methodologies and requiring significant resources. However, a review would provide an opportunity to assess the approaches which were applied and identify what improvements could be implemented for reliable continuous mapping over large scales in the future. Mapping approaches are driven not only by data needs, but by available technologies. In the marine environment, the opportunities afforded by new technologies such as machine- and deep-learning are rapidly expanding and opening new horizons toward improved seagrass mapping.

In this paper, we explored how seagrass mapping within the GBRWHA has been conducted previously, examined the approaches and limitations, and evaluated new technologies available to improve efficiency (including cost) and accuracy using a series of case studies. To examine new approaches and, where possible, compare with traditional approaches, we selected a variety of seagrass habitats and conditions as case studies to conduct trials. Using a critical evaluation, we also recommend a number of improvements to existing approaches and a future way forward.

## 2. Materials and Methods

### 2.1. Study Area

Stretching more than 2300 km along the Queensland coast, Australia, the Great Barrier Reef WHA is the most extensive reef system in the world, sheltering over 2800 individual coral reefs (derived from geomorphic map data down to 20 m depth [24]) and including 347,800 km<sup>2</sup> of seabed which supports extensive areas of seagrass of global significance [5,10].

Fifteen seagrass species are reported within the GBRWHA [5]: from just above mean sea level to 76 m deep [8]. They occur in 12 habitat types based on water quality types (estuary, coastal, reef, and offshore) and water depths (intertidal, shallow subtidal <15 m, and deep subtidal >15 m) (Table 1).

**Table 1.** Seagrass habitats of the GBRWHA and the composite seagrass extent. For seagrass habitat type description, see [25]. Seagrass extent from [7,10,26,27], where \* refers to modelled data.

Seagrass Habitat Type	Area (km <sup>2</sup> )	Percentage of Total Extent
Estuary intertidal	85.0	0.2
Estuary shallow subtidal	36.5	0.1
Estuary deep subtidal	0.2	0.001
Coastal intertidal	352.2	1.0
Coastal shallow subtidal	2080.5	5.8
Coastal deep subtidal	2811.9 *	7.9 *
Reef intertidal	213.5	0.6
Reef shallow subtidal	83.2	0.2
Reef deep subtidal	10,168.7 *	28.5 *
Offshore intertidal	18.4	0.1
Offshore shallow subtidal	37.6	0.1
Offshore deep subtidal	19,791.2 *	55.5 *
<b>Total</b>	<b>35,679</b>	

The most extensive areas of seagrass are reported to occur in the deep subtidal habitats (water >15 m depth) (Table 1); however, these seagrasses are relatively sparse, composed of colonising species, highly dynamic, and not as productive as shallower seagrass

habitats [28–30]. Intertidal and shallow subtidal seagrass habitats are generally denser and composed of more foundational species [21]. However, these habitats are also predominantly inshore where they are significantly influenced by seasonal and episodic pulses of sediment-laden, nutrient-rich river flows, resulting from high volume summer rainfall [31,32]. Cyclones, severe storms, wind and waves as well as macrograzers (e.g., fish, dugongs, and turtles) influence all habitats in this region to varying degrees [32]. As inshore seagrasses are under the greatest pressure [33], they are generally prioritized for assessments, to provide an understanding of their current state and an evidence base for coastal management policy and planning.

Intertidal and shallow subtidal seagrass habitats provide the greatest opportunity for assessments, with their relative ease in accessibility compared to deep, open water habitats. However, the inshore waters of the GBRWHA are optically complex [34], with varying degrees of water clarity which can limit the types of mapping approaches and observing platforms available. Therefore, mapping the seagrasses within the GBRWHA has many challenges, necessitating a hierarchical approach from fine-scale in situ field point observations to broad-scale habitat suitability modelling.

## 2.2. Desktop Assessment of Seagrass Mapping in the GBRWHA to Date

To examine the different approaches that have been implemented to map seagrass meadows/habitats within the GBRWHA, we conducted a systematic review. We used the preferred reporting items for systematic reviews and meta-analyses (PRISMA) (Figure S1) framework and protocols [35].

An electronic literature search was first performed from the published literature. We used Web of Science, PubMed (MEDLINE), and Google Scholar as the primary sources for the searches. We also conducted broader searches to acquire additional literature (thesis, technical and consultancy reports) including gray literature, freely accessible seagrass data portals, and authors' personal data collections. The primary database searches extended from 1965 to 2021 and included keywords (exclusively in English) related to occupants ("seagrass", OR "sea-grass"), AND map variants ("map", OR "distribution", OR "extent", OR "spatial"), AND location (v.g. "Great Barrier Reef", OR "GBR") OR state name (v.g. "Queensland", OR "QLD"), OR specific habitat names (v.g. "coastal", "reef", OR "intertidal", OR "deepwater"). In total, 1118 records were identified (Table S1).

In the initial phase, titles and abstracts were screened to identify potential mapping studies within the study area. In the second phase, full texts of the remaining articles were read to identify if they met the inclusion and exclusion criteria, e.g., included mapping of seagrass. We included studies and datasets that reported vector (including modelled) and raster data presented in an illustrative format.

Each eligible study and dataset was then gleaned for information on the approach used to capture the data and construct the final map. Information included: date and location of each mapping event; mapping scale and organisation spatial level (Table 2); area of interest; the earth observing elements and instruments employed for data capture (Table 3); survey method, type of field validation and measures; type of habitat, seagrass species present; meadow type, form, and arrangement/organisation (meadow-scape); how the map was constructed; and the accuracy of the data collected and maps created (Table S1). We defined remote sensing as the gathering of information about objects or areas without making direct physical contact with the object.

We used the results of the systematic review to identify temporal and spatial trends in seagrass mapping approaches within the GBRWHA and its habitats. To spatially quantify seagrass mapping, each mapping event was overlaid and allocated to 30 min grid cells (30 nautical miles  $\times$  30 nautical miles) [36].

We used a multicriteria analysis approach to semiquantitatively score the confidence of the mapping product from each mapping event reviewed (Table 4). The criteria (Table S2) and the approach used follows the method successfully implemented for the Paddock to Reef integrated monitoring, modelling and reporting program [37]. Each criterion was

scored, by an expert, using a defined set of scoring attributes (Table 4). The determination of confidence for each mapping product used five criteria: maturity of methodology, validation, representativeness, directness, and measured error. For maturity of methodology, the score was weighted half for this criterion so as not to outweigh the importance of the other criteria. The strength of this approach is that it is repeatable, transparent, and can include contributions from a range of sources.

**Table 2.** Seagrass organisation form, spatial scale, temporal scales, and features measured. Spatial scale = maximum and minimum area covered by seagrass organisation form; Temporal scale = time scale on which the seagrass organisation form undergoes changes; Measures = features of the seagrass organisation form able to be measured. Modified [38].

	Seagrass Organisation	Spatial Scale	Temporal Scale	Examples of Measures
Fine (micro)-scale	Patch/Patches	1–100 m	Weekly, monthly, annual	Areal extent, abundance per unit area (photoquadrats, percent cover and/or biomass, shoot density), species, shoot height, rhizome biomass, reproductive health (flower, fruit, and seed abundance), macroalgae abundance
	Meadow	100 m–1 km	Seasonal (3–4 months) to annual	Areal extent, meadow-scape, abundance per unit area (photoquadrats, percent cover and/or biomass), species, reproductive health (flower, fruit, and seed abundance), macroalgae abundance
Meso-scale	Meso-system meadows e.g., small bay/estuary	1–10 km	Seasonal (3–4 months) to annual, decadal	Areal extent, meadow-scape, abundance (per unit area), species presence/absence, macroalgae abundance
	Subregional meadows e.g., large bay	10–50 km	Seasonal (3–4 months) to annual, decadal	Areal extent (presence/absence), meadow-scape (categories), abundance (per unit area)
	Regional meadows e.g., large island group	50–100 km	Biannual to annual, decadal	Areal extent (presence/absence), meadow-scape (categories), abundance (narrow categories)
Broad (macro)-scale	Biome meadows (e.g., dry tropics, wet tropics, NRM region)	>100 km	decadal	Areal extent (presence/absence), meadow-scape (categories), abundance (broad categories)

**Table 3.** Earth observing elements including type and data capture approach. Effective resolution is the size of the smallest feature that is discernible. Spatial extent per observation refers to maximum resolvable area represented by a single measure/capture.

Observing Type	Definition	Effective Resolution	Temporal Resolution	Approach/Instrument	Spatial Extent per Observation
Direct in situ	Measures taken directly from the object/feature, i.e., within human reach.	<3 m	On-demand to seasonal	by foot; diver (free, SCUBA)	10 m <sup>2</sup>
	Measures taken directly from the object/feature via a device, i.e., beyond human reach.	≥3 ≤10 m	On-demand to seasonal	grab, rake, sled	100 m <sup>2</sup>

Table 3. Cont.

Observing Type	Definition	Effective Resolution	Temporal Resolution	Approach/ Instrument	Spatial Extent per Observation
Near Earth Observing	Active and passive remotely sensed data collected from submerged sensors at a depth beyond human reach.	$10^{-2} \leq 10$ m	On-demand to seasonal	camera (drop-camera, Closed-Circuit Television), Autonomous Underwater Vehicle (AUV), helicopter, acoustic (from a boat).	100 m <sup>2</sup>
High Earth Observing	Near-field passive remotely sensed data collected from airborne sensors at an altitude >10 m above the object/feature.	$10^{-3} \leq 100$ m	On-demand to monthly to biannual	Unoccupied Aerial Vehicle (UAV), Unoccupied Aerial Systems (UAS), helicopter, fixed wing aircraft	5 ha
Earth Observing from Space	Passive remotely sensed data collected from spaceborne sensors, at an altitude >10 <sup>5</sup> m above the object/feature.	$\sim 1 \leq 100$ m	On-demand to 1 to 10 days [39]	satellite, spacecraft	185 km <sup>2</sup>

Table 4. Mapping confidence scoring matrix. Confidence scoring and categories used: very low,  $\leq 5$ ; low,  $>5 \leq 7.5$ ; moderate,  $>7.5 \leq 10$ ; high,  $>10 \leq 12$ ; very high,  $>12$ . Criteria are weighted relative to their perceived level of importance for the assessment being addressed. Modified [37]. Scales and effective resolution adapted from [40–42], ancillary attributes from [43,44].

Maturity of Methodology (Weighting = 0.5)	Validation (Observing Platforms) (Weighting = 1)	Representativeness (AOI) (Weighting = 1)	Directness (Mapping Approach) (Weighting = 1)	Measured Mapping Error (Weighting = 1)
Score = 1 <ul style="list-style-type: none"> <li>new or experimental methodology</li> <li>limited use</li> <li>pre-1980s methodology</li> </ul>	Score = 1 <ul style="list-style-type: none"> <li>no field validation. or field validation &gt; 6 months from image acquisition</li> <li>in situ sampler/grab</li> <li>Spaceborne or airborne observing (high altitude, low resolution)</li> </ul>	Score = 1 <ul style="list-style-type: none"> <li>less than 10% of AOI assessed</li> <li>prediction area &gt; 10 times larger than validation area</li> </ul>	Score = 1 <ul style="list-style-type: none"> <li>on screen interpolation of air- or spaceborne imagery</li> <li>remotely sensed, high altitude, low resolution</li> <li>raster resolution &gt; 10 m</li> <li>modelled habitat suitability</li> </ul>	Score = 1 <ul style="list-style-type: none"> <li>error not measured or stated</li> <li>scale &gt; 1:100,000</li> <li>effective resolution 100–500 m</li> <li>&lt;40% correct classification</li> <li>&lt;40% Bootstrap Probability</li> </ul>
Score = 2 <ul style="list-style-type: none"> <li>peer reviewed method (not formally published)</li> <li>used for &gt;10 years</li> <li>improvement of existing method</li> </ul>	Score = 2 <ul style="list-style-type: none"> <li>survey with some field-validation or field validation 1 to 6 months from image acquisition</li> <li>direct in situ measures, but unvalidated (e.g., no photquadrats)</li> <li>Near earth observing</li> <li>High earth observing (helicopter or high alt UAV)</li> </ul>	Score = 2 <ul style="list-style-type: none"> <li>10–50% of AOI assessed</li> <li>assessment clumped throughout AOI</li> <li>prediction area 5–10 times larger than validation area</li> </ul>	Score = 2 <ul style="list-style-type: none"> <li>on screen human interpolation from in situ data</li> <li>field based boundary mapping from helicopter</li> <li>remotely sensed, high altitude, med-high resolution</li> <li>raster resolution &gt; 3 m <math>\leq</math> 10 m</li> </ul>	Score = 2 <ul style="list-style-type: none"> <li>&gt;10-fold field accuracy</li> <li>scale <math>\leq</math> 1:10,000 to 1:100,000</li> <li>effective resolution &gt; 10 to <math>\leq</math> 100 m</li> <li>40–70% correct classification</li> <li>meadow-scape categorised</li> <li>&gt;40% &lt;60% Bootstrap Probability</li> </ul>
Score = 3 <ul style="list-style-type: none"> <li>globally standardised (e.g., [45]), peer reviewed and used in a number of peer reviewed publications</li> <li>analysed following well published methods</li> </ul>	Score = 3 <ul style="list-style-type: none"> <li>direct in situ human-geotagged photoquadrats or geolocated quadrat observations</li> <li>high earth, low altitude UAV, high resolution</li> <li>field validation within 1 month of image acquisition</li> <li>modelling with comprehensive validation &amp; supporting documentation</li> <li>supported by expert knowledge</li> </ul>	Score = 3 <ul style="list-style-type: none"> <li>&gt;50% of AOI assessed</li> <li>assessment spread throughout AOI</li> <li>similar sized prediction and validation areas</li> <li>expert knowledge of data source for AOI</li> </ul>	Score = 3 <ul style="list-style-type: none"> <li>field based boundary mapping on foot</li> <li>remotely sensed, low altitude, high resolution (e.g., UAV)</li> <li>raster resolution <math>\leq</math> 3 m</li> </ul>	Score = 3 <ul style="list-style-type: none"> <li>similar to field accuracy</li> <li>scale &lt; 1:10,000</li> <li>effective resolution <math>\leq</math> 10 m</li> <li>&gt;70% correct classification</li> <li>meadow-scape measured (patches, scars)</li> <li><math>\geq</math>60% Bootstrap Probability</li> </ul>

### 2.3. Applied Assessment of Traditional and Enhanced Mapping Approaches

Approaches to mapping seagrass were conducted and compared through three case studies, each focusing on a different area of interest (AOI), to demonstrate possible improvements to mapping the diverse and dynamic seagrass meadows of the GBR.

#### 2.3.1. Characteristics of Case Study Areas

The selected case studies included a variety of seagrass habitats (coastal, reef, intertidal, and shallow subtidal) and conditions (clear and optically complex waters) experienced in the GBRWHA (Table 5, Figure 2). The AOIs included the most commonly mapped habitats within the GBRWHA, and have been monitored as part of the Seagrass-Watch and the Great Barrier Reef Marine Monitoring Program (MMP) for over 15 years [21]. The AOIs also included seagrass communities with abundances representative of the GBRWHA historic baseline,  $22.6 \pm 1.2\%$  cover (mean  $\pm$  SE) [46] (Table 5).

**Table 5.** Case study (see Figure 2) including coordinates (midpoint, geographic name), observing platform, habitat (including description of sediment grain size, colour and origin), and seagrass community (incl. long-term percent cover from 2000 to 2020).

Case Study (Coordinates, Name)	Observing Platform (Data Capture Date)	Habitat Type (Sediment)	Seagrass Community (Mean Cover $\pm$ SE)
Coastal clear water (16.564°S, 145.511°E) Yule Point	Direct in situ (by foot) (15 October 2017, 13–14 August 2019, 6 September 2020) Airborne (UAV) (20 July 2020) Airborne (helicopter) (5 September 2017) Spaceborne (satellite) (5 September 2017, 9 August 2019)	coastal intertidal/ shallow subtidal (fine sand, light coloured, terrigenous)	<i>Halodule uninervis</i> , <i>Halophila ovalis</i> (15.0 $\pm$ 1.6% cover)
Coastal turbid water (20.635°S, 148.709°E) Midge Point	Direct in situ (by foot) (17 September 2017) Airborne (helicopter) (17 October 2017) Spaceborne (satellite) (9 October 2017)	coastal intertidal/ shallow subtidal (mud/fine sand, dark coloured, terrigenous)	<i>Zostera muelleri</i> , <i>Halodule uninervis</i> (24.9 $\pm$ 1.8% cover)
Reef clear water (16.762°S, 145.976°E) Green Island (Wunyami)	Direct in situ (by foot) (25–27 November 2020) Airborne (UAV) (25 November 2020) Spaceborne (satellite) (5 November 2020)	reef intertidal/ shallow subtidal (coarse sand/sand, light coloured, biogenous-37% CaCO <sub>3</sub> )	<i>Thalassia hemprichii</i> , <i>Halodule uninervis</i> , <i>Syringodium isoetifolium</i> , <i>Cymodocea serrulata</i> , <i>Cymodocea rotundata</i> , <i>Halophila ovalis</i> (36.4 $\pm$ 2.2% cover)

#### 2.3.2. Data Collection and Mapping for Case Studies

We conducted four mapping approaches in the case studies by, first, using the most common traditional approaches to collect data and create maps that have been applied across the GBRWHA over the last century, and then using new technologies of image capture and machine- and deep-learning.

##### Approach 1: Field-Based Direct In Situ Boundary Track (by Foot)

###### Data used

Sections of AOIs were mapped during low spring tides. These sections (e.g., sites) covered an area of approx. 5.5 hectares, and field survey methodology followed globally standardised protocols (detailed in [45,47]). Mapping of the meadowscape (including patches and scars) was conducted on foot using a handheld Garmin GPSMap 64s (accuracy  $\pm$ 1.5–3 m).

### Mapping method

The GPS tracks were imported into ESRI® ArcMap™ 10.7 (Environmental Systems Research Institute, ArcGIS™ Desktop 10.7). Meadowscape (patches or scars) boundaries were mapped using the imported GPS track to create a polyline which was then smoothed using the B-spline algorithm and saved as a polygon.

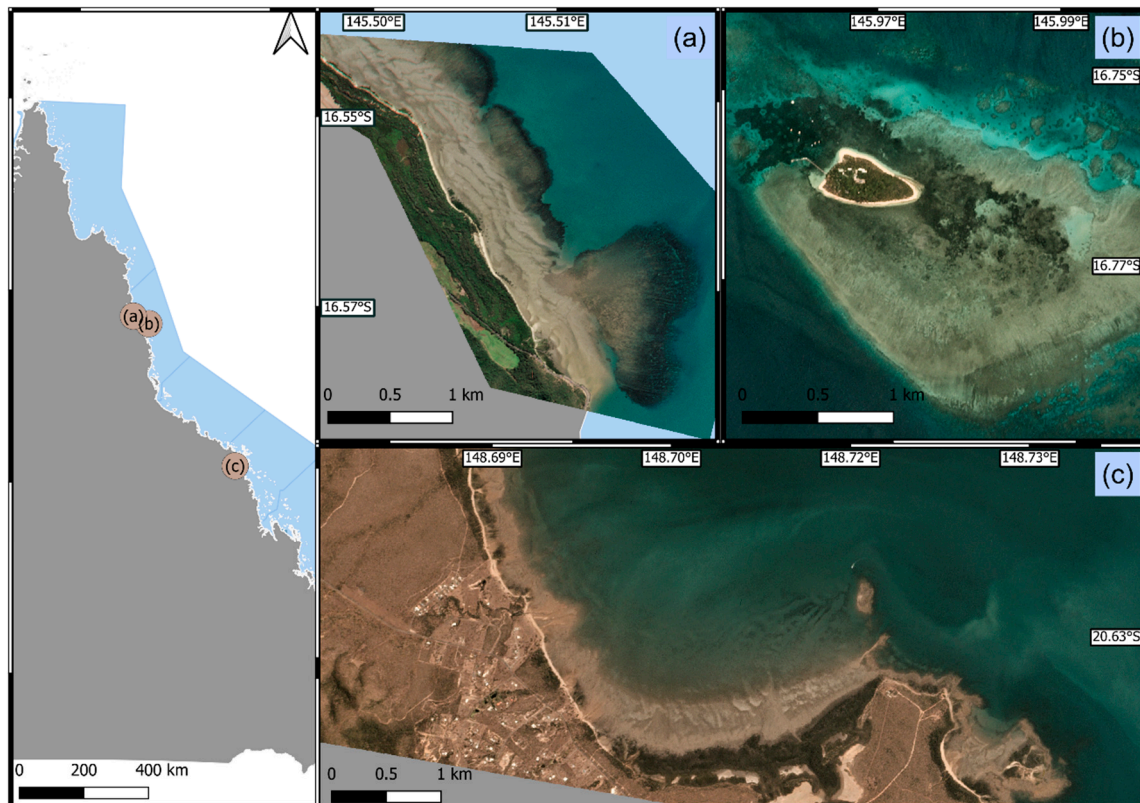


**Figure 2.** Location of each case study: (a) coastal clear water (Yule Point); (b) reef clear water (Green Island); and (c) coastal turbid water (Midge Point).

### Approach 2: Field-Based Direct In Situ Spot-Check and High Earth Boundary Track (by Helicopter)

#### Data used

The coastal seagrass meadows (Yule Point and Midge Point) were surveyed at low tide with observations from a helicopter (Robinson R44/R66). The boundaries of the meadows were delineated by onboard observers and tracked by helicopter (at  $25 \pm 5$  m altitude) using the tracks setting on a handheld Garmin GPSMap 64s. Within these meadows, observational data was collected at an altitude of 1–2 m above the substrate, from three haphazard placements of a  $0.25 \text{ m}^2$  quadrat out the side of the helicopter at a number of haphazardly scattered points (spot-checks,  $10 \text{ m}^2$ ) (Figure S2). Seagrass species were verified using an extendable cultivator rake to collect shoots. The boundaries of the reef seagrass meadows were mapped by foot as aircraft are restricted within the Green Island Marine National Park [48].

#### Mapping method

All field survey data were imported into ESRI® ArcMap™ [49] and seagrass meadow boundaries mapped from the GPS tracks and by onscreen interpolation based on geolocated spot-checks (Figure S2), field notes, and geotagged oblique aerial photographs acquired from the helicopter. Meadow area was determined using the calculate geometry function in ArcGIS®. The mapping precision using this mapping approach was set at  $\pm 10$  m either side of the interpreted meadow boundary, taking into account errors associated with the GPS and the altitude of the helicopter. A mapping precision estimate was used to calculate a

buffer around each meadow (using the buffering function) representing error; the meadow area excluding and including this buffer is expressed as a meadow reliability estimate in hectares [45].

### Approach 3: High Earth Mapping with Unoccupied Aerial Systems (UAS) Captured Imagery

#### Data used

UAS imagery was collected with a DJI Mavic 2 Pro unoccupied aerial vehicle (UAV) at the coastal clear water and reef clear water AOIs during low spring tides (Table 5). The UAS used DroneDeploy to manage the UAV at an altitude of 30 m and 100 m in coastal and reef habitats, respectively (85% sidelap and frontlap). The captured images from each altitude were meshed into orthomosaics in PIX4D and their resolutions were 0.2 cm/pixel and 2.45 cm/pixel, respectively.

#### Mapping method

We created spatially explicit seagrass maps from UAS acquired nadir imagery using deep-learning techniques, see basic workflow Figure 3a (Supplementary Material S3). The orthomosaics from the coastal clear water (Yule Point,  $57,332 \times 57,238$  pixels,  $\sim 1.31$  ha) and reef clear water (Green Island,  $10,098 \times 7444$  pixels,  $\sim 4.51$  ha) AOIs were decomposed into  $256 \times 256$  pixel tiles to be used in deep-learning. A proportion of both the coastal and reef tiles (0.8% and 29%, respectively) were manually annotated and assigned a seagrass abundance class (supervised) for training, testing, and validation. This was performed in the web-based annotation platform Labelbox [50].

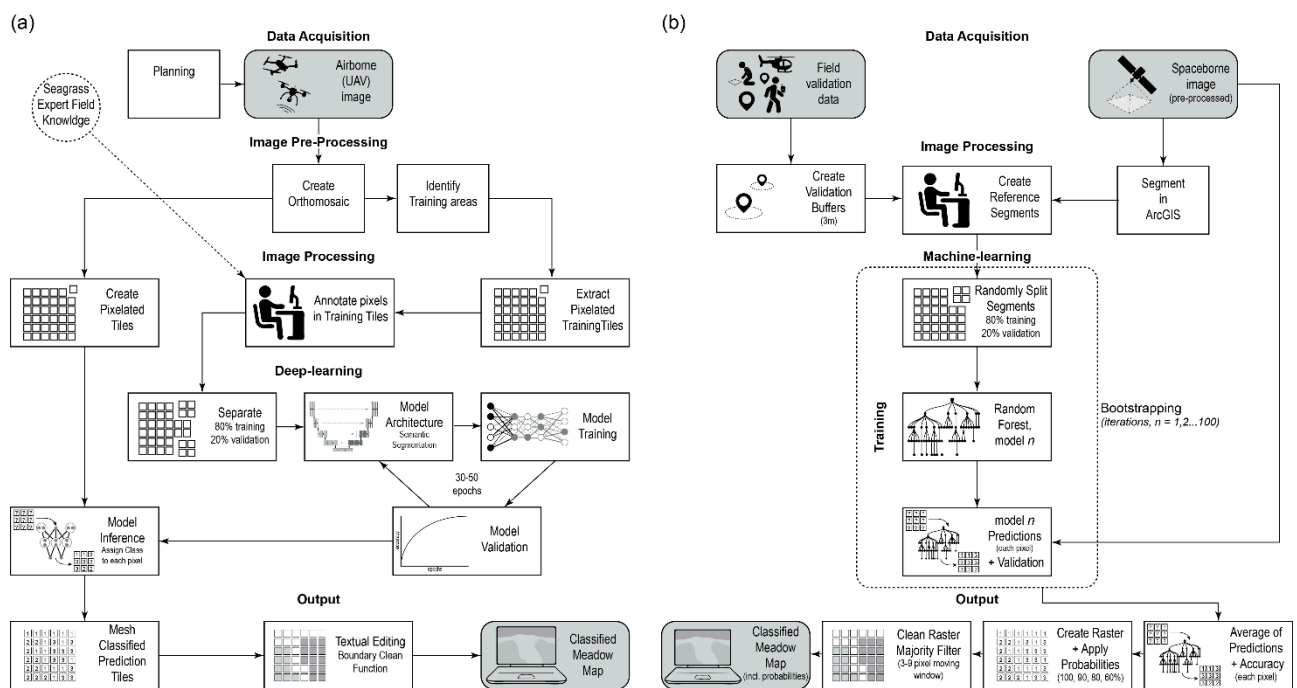


**Figure 3.** The general workflow of optical imagery acquired by UAV (a) and spaceborne sensors (b), illustrating the image processing and application of deep- and machine-learning (a and b, respectively) to produce spatially explicit classified seagrass meadow maps.

For the coastal AOI, due to the lower seagrass density and occurrence of morphologically smaller species, the classes used were: (1) bare sediment, (2) low seagrass cover ( $>0 \leq 25\%$ ), (3) high seagrass cover ( $>25\%$ ), (4) rubble/algae. For the reef AOI, the classes used were: (1) absence of seagrass (0%), (2) low seagrass cover (1–15%), (3) medium seagrass cover ( $>15-50\%$ ), and (4) high seagrass cover ( $>50\%$ ). The resulting annotations were fairly evenly spread across classes for the coastal (29, 28, 25, and 17%, respectively), but were more unbalanced for the reef (1, 17, 34, and 47%, respectively).

#### Approach 4: Earth Observing from Space with Satellite Captured Imagery

##### Data used

PlanetScope Dove, with  $3.7\text{ m} \times 3.7\text{ m}$  pixels (nadir viewing) with RGB (red, green, blue) and for some sensors also half NIR (near-infrared) [51] was acquired from the PlanetScope archive [52]. This imagery is captured daily as a result of a constellation of 170+ dove cube satellites. With Blue band 455 nm to 515 nm, green 500 nm to 590 nm, red 590 nm to 670 nm, NIR 780 nm to 860 nm [51]. Imagery was provided orthorectified and radiometrically corrected to surface reflectance (SR) product [51]. We acquired PlanetScope images coinciding as close as possible to the field-surveys in 2017, 2019, and 2020 (Table 5). Field validation data in 2019 and 2020 was collected by foot at haphazard points or along transects perpendicular to the shoreline (Figure S4). At each point a geotagged photograph of the benthos ( $1\text{ m} \times 1\text{ m}$ ) was captured using a GoPro HERO9 Black or Olympus TG5.

##### Mapping method

We created spatially explicit seagrass maps from the imagery, and conducted the classification in R [53] using a machine-learning model (random forest) with the ranger package [54]. The basic workflow is shown in Figure 3b (see also Supplementary Material S3). Classified polygons (reference segments) were created by segmenting the image in ArcGIS Pro [55] and then manually assigning a label through expert interpretation of the imagery and field data (Figures S2–S4). We used an 80–20% random split of the classified pixels to train and validate the model, respectively [56]. This process was repeated over 100 iterations for which each model output metrics (out-of-bag (OOB) error rate, class error rate, and validation accuracy) and model predictions for the whole image were compiled by taking the average. This method, known as bootstrapping, had the advantages of making sure the random split was not leading to a biased model (e.g., if unique classified segments are low or if the segments are too large and heterogeneous) and that each pixel prediction had a probability associated to it. The final model predictions were then gathered into separate rasters, based on four bootstrap probability thresholds: 100, 90, 80, and 60%. The final rasters were cleaned using a majority filter algorithm, to eliminate stray pixel predictions in R (focal function from raster package) using a moving window between 3 and 9 pixels depending on the size of the imagery.

#### 2.3.3. Comparison of Mapping Approach Outputs

To compare the different mapping approaches and enhancements, we assessed the output maps created at both fine- (patch to meadow) and meso-scales (meso-system meadows). We compared the areas of seagrass mapped (in hectares, including reliability, probability, and confidence) and meadow characteristics (including abundance and meadowscape) using each approach and type of observing platform, within each of the different seagrass habitats (case studies).

### 3. Results

#### 3.1. Desktop Assessment of Seagrass Mapping in the GBRWHA to Date

We identified 395 individual seagrass mapping events having occurred within the GBRWHA up until December 2020 (Table S1). The earliest verified record of seagrass within the GBRWHA was in 1802 [3]; however, the inclusion of seagrass in maps did not appear until 1931 when reef flat *Thalassia* and *Halophila* habitats were mapped at Low Isles during the Great Barrier Reef Expedition 1928–1929 [57,58]. In the decades following, maps of seagrass were small scale and principally research focussed. The first broadscale inventory of the seagrass meadows of the GBR was achieved within the 1980s (Table S1). Since then, seagrass mapping has continued at various scales and has been predominately driven by management needs. The accessibility to Geographic Information Systems (GIS) and digital imaging has also progressed cartography beyond paper maps to a digital format, enabling maps to be created by a wider variety of actors for an even greater diversity of users.

### 3.1.1. Earth Observing Platforms and Mapping Approaches

The most popular observing platform employed to create maps of seagrass meadow extent within the GBRWHA was in situ human (84% of mapping events), followed by in situ sampler, high earth, near earth, and spaceborne, respectively (Figure 4a).

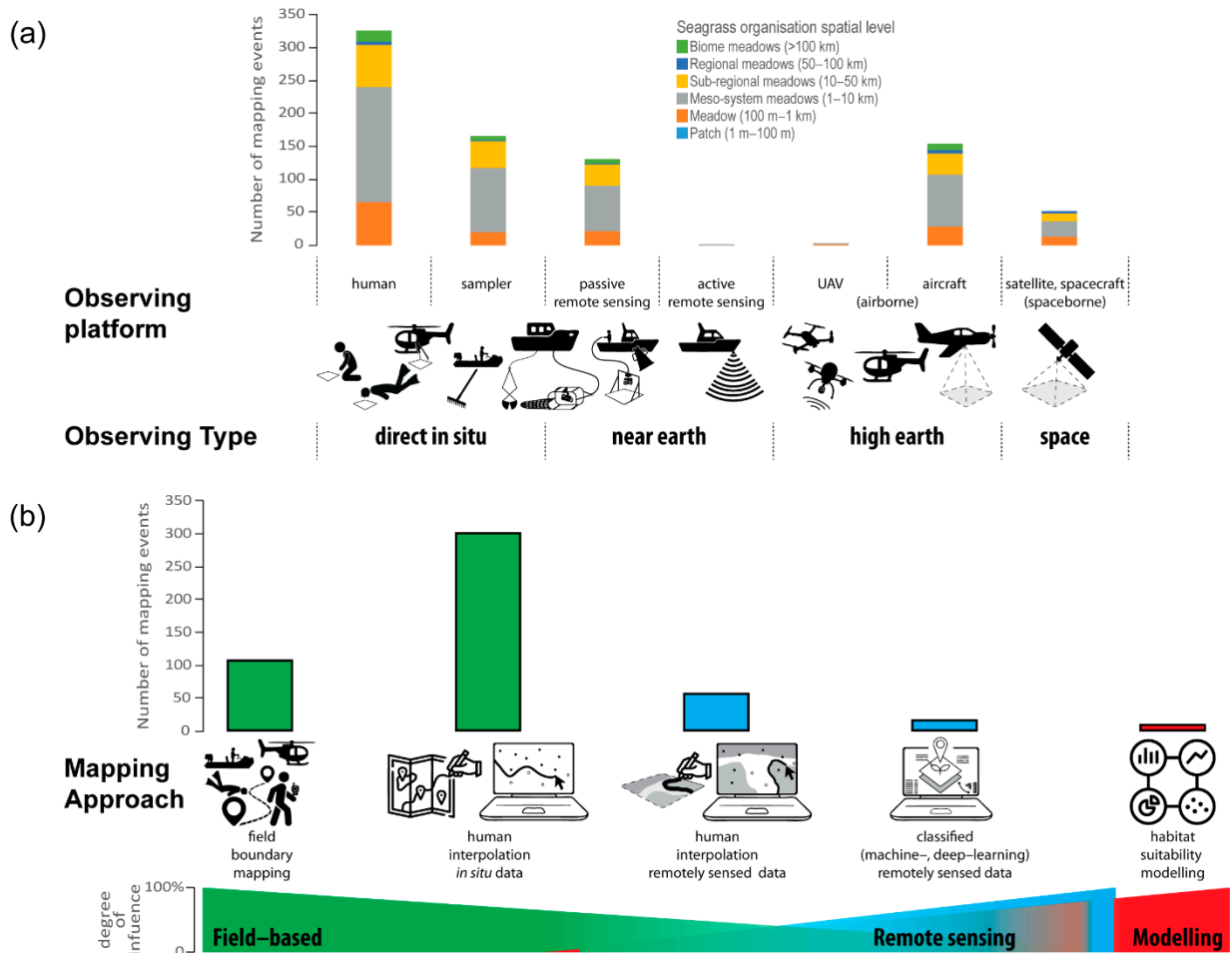


**Figure 4.** Frequency of occurrence of each earth observing platform type and seagrass organisation spatial level (a), and mapping approach (b) used to map seagrass meadows within the GBRWHA over the last century (1920–2020). The degree of influence illustrates the contribution of each broad grouping to specific mapping approaches: green = field-based, blue = remote sensing, and red = modelling. See Table 2 for seagrass organisation level and Table 3 for observing platform and type. Source data provided in Table S1.

Within the GBRWHA, a number of approaches have been used to map seagrass meadows, varying from field-based to habitat suitability modelling (Figure 4b). The approaches can include in situ field-validation methods which range from direct human observation to remote sensing. Field-based approaches dominated across the mapping events (Figure 4b), with onscreen interpolation and hand-digitisation of meadow boundaries by the user (based on the presence or absence of seagrass at a field validation point, e.g., spot-check and expert interpretation) being the most popular cartographic technique. These approaches have been mostly applied at the meso-system meadows organisational level (Figure 4a).

Although approximately 40% of mapping events included high earth observing, this was for the most part where aerial photographs (from fixed wing aircraft) were used only to assist with the map presentation (e.g., background).

Earth observing from space was reportedly used in 14% of mapping events; however, similar to the high earth, these were predominately only to visually assist with human

interpolation, and images were not classified. Attempts to use classified spaceborne imagery to map inshore seagrass meadows on the GBR were first reported in 1980–1981, however, these were hampered by the coarse spatial resolution (e.g., 80 m) of the scanner and the poorer spectral range [59]. Since that time, we found only five events (excluding the present study) where spaceborne imagery, coupled with field validation data, has successfully produced a spatially explicit seagrass map within the GBRWHA (Table S1). Similarly, we found only three events where habitat suitability modelling, using supervised machine-learning methods, has produced spatially explicit seagrass maps (Table S1). Both of these approaches were only successfully applied in the last decade (2010–2020).

### 3.1.2. Mapping Characteristics

Mapping events were geographically focussed predominantly to the inshore waters of the GBRWHA, with the greatest frequency associated with industrial ports and urban centres (Figure 5). A disproportionate number of sampling events (27%) mapped seagrass in the vicinity of Cairns (Figure 5) relative to other locations within the GBRWHA.

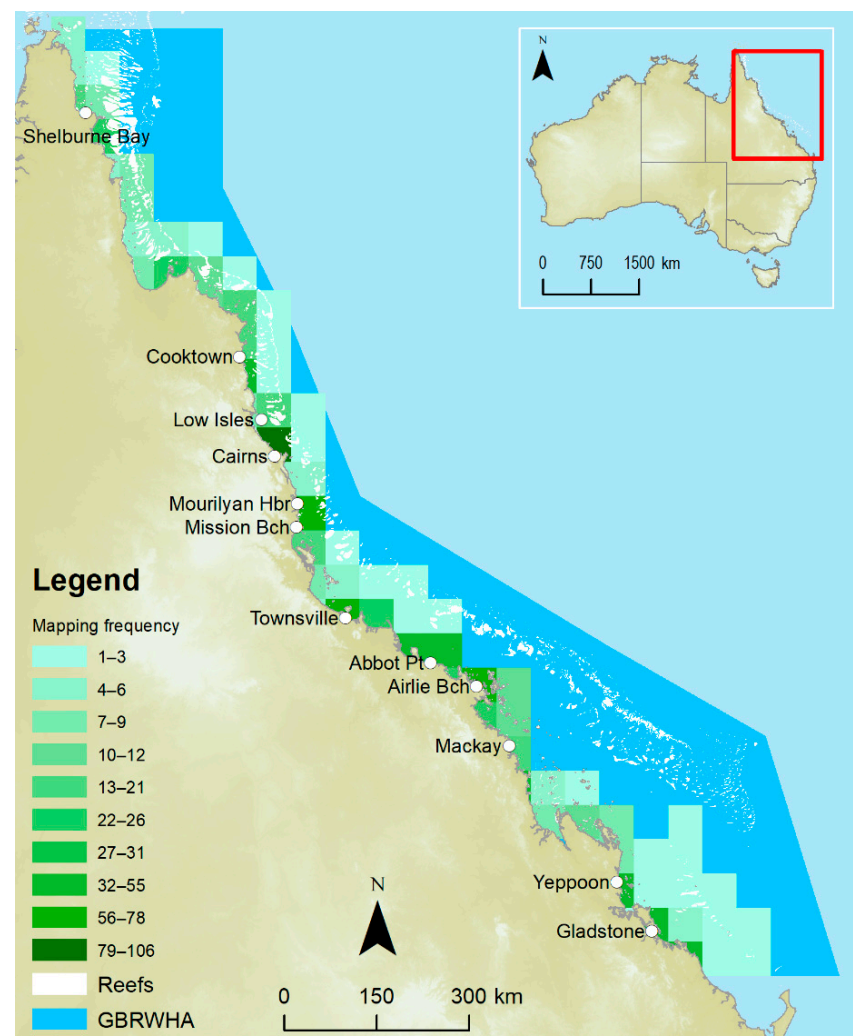


**Figure 5.** Frequency of seagrass meadow mapping events, within 30 min grids, within the Great Barrier Reef World Heritage Area over the last century (1920–2020).

The mapping of seagrass meadows within the GBRWHA shows a temporal bias—an unbalanced occurrence of mapping in some years or parts of a given year (Figure 6). Historic mapping events (pre-1960) were generally during the lowest daytime spring tides, which occur toward the middle of each calendar year along the Queensland east coast

(Figure 6a). Post-1960s, mapping gradually spread throughout the year, and from the mid-1990s, was biased more toward the latter months of the year, peaking in November (Figure 6a). Two-thirds of the mapping events occurred during the austral growing season (August–January for most Australian tropical seagrass species) (Figure 6a). Temporal trends in seagrass mapping were also not consistent across seasons within each of the marine Natural Resource Management regions (NRMs) of the GBRWHA (Figure 6b).

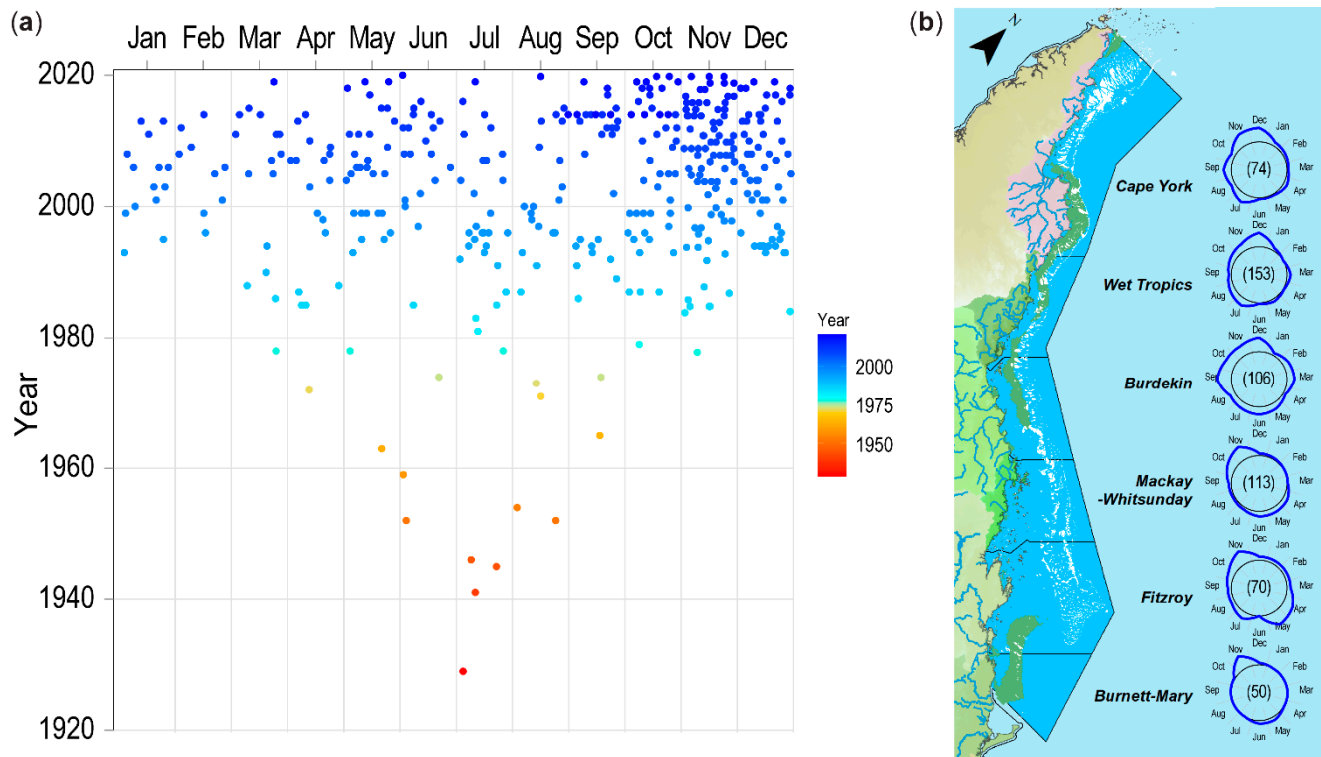


**Figure 6.** Temporal occurrence in seagrass meadow mapping events within the Great Barrier Reef World Heritage Area: (a) within and across years, where each dot represents a mapping event, with the colour gradient representing recent years with colder colour tones, and older years represented by warmer colour tones; (b) intra-annual trends within each Natural Resource Management region, where the blue line around each temporal plot represents mapping frequency in monthly intervals (scaled to monthly maximum) over the last century (1920–2020) and the value in the centre of each plot is the total number of mapping events. Source data are provided in Table S1.

Mapping events were biased to intertidal and subtidal coastal habitats of the GBRWHA, particularly in the last three decades (Figure 7). Conversely, offshore habitats were the least mapped over the last century, occurring mainly in the 1980s and 1990s (Figure 7).

### 3.1.3. Mapping Confidence

Confidence for the maps of seagrass meadow extent produced by the mapping events varied depending on the habitats, observing platforms, and approach (Table S2). Approximately half (49%) of the mapping events produced seagrass extent maps of moderate confidence. These mapping events followed standardised approaches, including sufficient field validation (e.g., in situ point assessments using helicopter, diver, camera, grab) with some measure of field accuracy, but meadowscapes were categorised rather than mapped and the meadow boundaries were visually interpolated and digitised by hand onscreen. Over a third of the mapping events produced maps of low to very low confidence, with only the remainder (14%) of high to very high confidence.

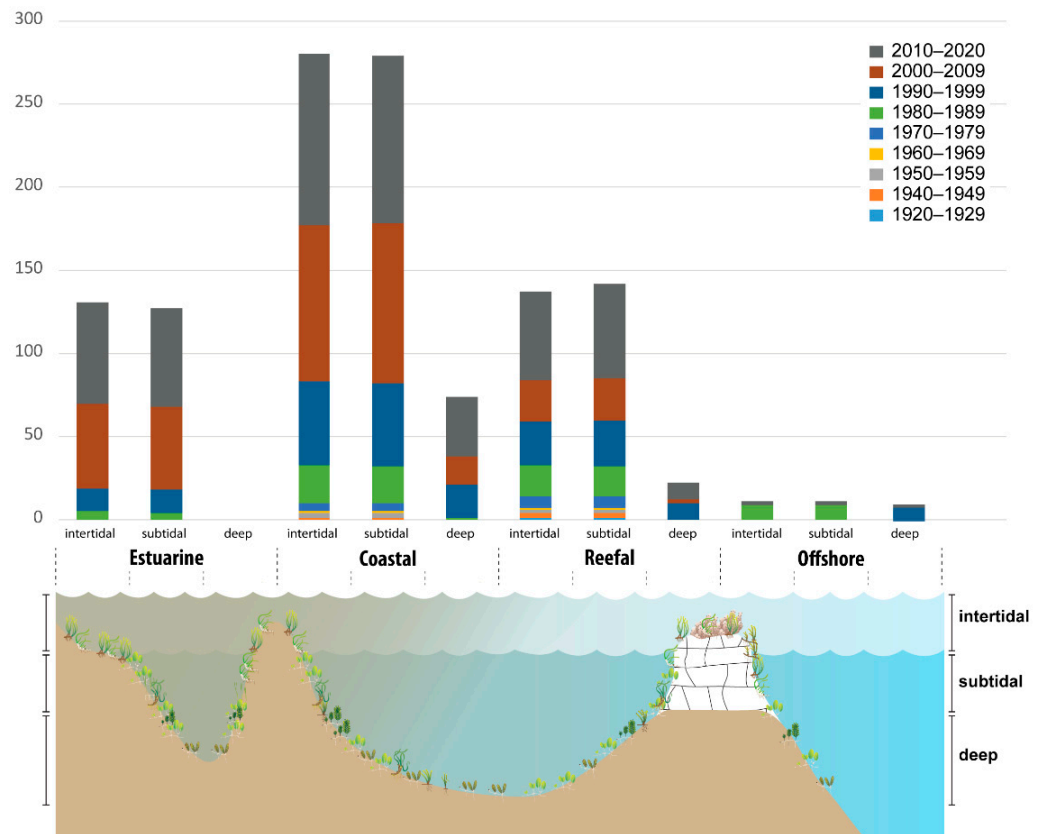


**Figure 7.** Number of events mapping seagrass meadow extent in each of the seagrass habitats across the GBRWHA over the last century (1920–2020). Conceptual diagram based on Udy et al. [25]. Source data are provided in Table S1.

### 3.2. Applied Comparison of Traditional and Enhanced Mapping Approaches

The case studies occurred within the two NRM regions which had the highest mapping frequency in the GBRWHA (Figure 6b) and included the most often mapped habitats: coastal and reef (see Figure 7).

#### 3.2.1. Fine-Scale Mapping—Patch to Meadow (AOI = 5.5 ha)

Traditional direct in situ boundary mapping by foot resulted in comprehensive maps of seagrass extent and meadowscape (patches and scars) of very high confidence, for both types of intertidal seagrass communities (Figure 8). Maps produced by high earth boundary mapping using a low flying helicopter, however, were of low confidence and lacked meadowscape details (e.g., scars and patches), especially in the *Zostera muelleri* dominated community (Figure 8). Mapping from spaceborne-captured imagery produced reasonably comprehensive maps of seagrass extent and meadowscape of high confidence, across both intertidal seagrass community types (Figure 8). The area of seagrass measured within the AOI was similar or slightly higher when mapped using spaceborne approaches compared to in situ boundary mapping by foot (Table 6). When using the spaceborne approach, the difference between the areas of seagrass mapped with either the 100% or 60% bootstrap probability threshold was less than 5% (Table 6). The areas of seagrass measured using a low flying helicopter were consistently higher than both the in situ field-based and spaceborne approaches, with the differences ranging from 11 to 55% and 3 to 102% greater, respectively (Table 6).

**Table 6.** Area of seagrass (hectares) mapped within each AOI in 2017 using different earth observing platforms and approaches to create fine- and meso-scale spatially explicit seagrass maps for coastal clear and turbid water habitats in the GBRWHA. The range in seagrass area is based on estimate of reliability (\*) or bootstrap probability. n.a. indicates a boundary could not be delineated within the AOI due to the type of earth observing platform used.

AOI	Mapping Scale	Site (ha)	Earth Observing Platform	Resolution or Bootstrap Probability	Seagrass Area	
					ha	Range
Coastal clear water (Yule Pt)	Fine-scale	YP1 (4.58)	Direct in situ—by foot	high	2.86	
			High earth—helicopter	low *	3.95	3.34–4.43
			Spaceborne—satellite	100% 60%	2.19 2.33	2.19–2.33
		YP2 (5.09)	Direct in situ—by foot	high	4.44	
			High earth—helicopter	low *	5.05	4.93–5.08
			Spaceborne—satellite	100% 60%	4.69 4.78	4.69–4.78
	Meso-scale	(193.08)	High earth—helicopter	low *	144.06	134.61–151.85
			Spaceborne—Satellite	100%	105.32	105.32–14.63
				90%	110.55	
				80%	112.45	
60%	114.63					
Coastal turbid water (Midge Pt)	Fine-scale	MP2 (5.27)	Direct in situ—by foot	high	4.7	
			High earth—helicopter	low *	5.268	n.a.
			Spaceborne—Satellite	100% 60%	4.43 4.48	4.43–4.48
		MP3 (5.27)	Direct in situ—by foot	high	4.89	
			High earth—helicopter	low *	5.268	n.a.
			Spaceborne—Satellite	100% 60%	4.76 4.78	4.76–4.78
	Meso-scale	(130.05)	High earth—helicopter	low *	117.79	114.36–120.93
			Spaceborne—Satellite	100%	96.68	96.68–100.44
				90%	98.88	
				80%	99.55	
60%	100.44					

### 3.2.2. Meso-Scale Mapping—Meso-System Meadows (AOI = 130 to 317 ha)

High earth boundary mapping using a low flying helicopter was able to cover the entire coastal AOIs within the tidal window and produce a map of seagrass meadow extent; however, the maps were of moderate confidence and lacked meadowscape details due to the low accuracy delineating boundaries of individual patches and scars (Figure 8). Spaceborne-captured imagery produced reasonably comprehensive spatially explicit maps of seagrass meadowscape of high confidence, across both coastal seagrass habitats (Figure 8). The average accuracy across the 100 random forest models produced were  $98.78 \pm 0.01$  and  $98.69 \pm 0.01$  at the coastal clear water and coastal turbid water meadows, respectively (Table S3). We found that the areas of seagrass measured in each AOI using a helicopter were consistently higher than when measured using the spaceborne approach, for both the 100% and 60% bootstrap probability thresholds (Table 6). No in situ boundary mapping by foot was possible at meso-scale due to the limited tidal window available (3–4 h) for access.

We found that high earth mapping using a helicopter consistently overestimated seagrass extent by 24.5% on average (range 6 to 80%), depending on the complexity of the meadowscape, i.e., the greater the complexity, the greater the overestimate.

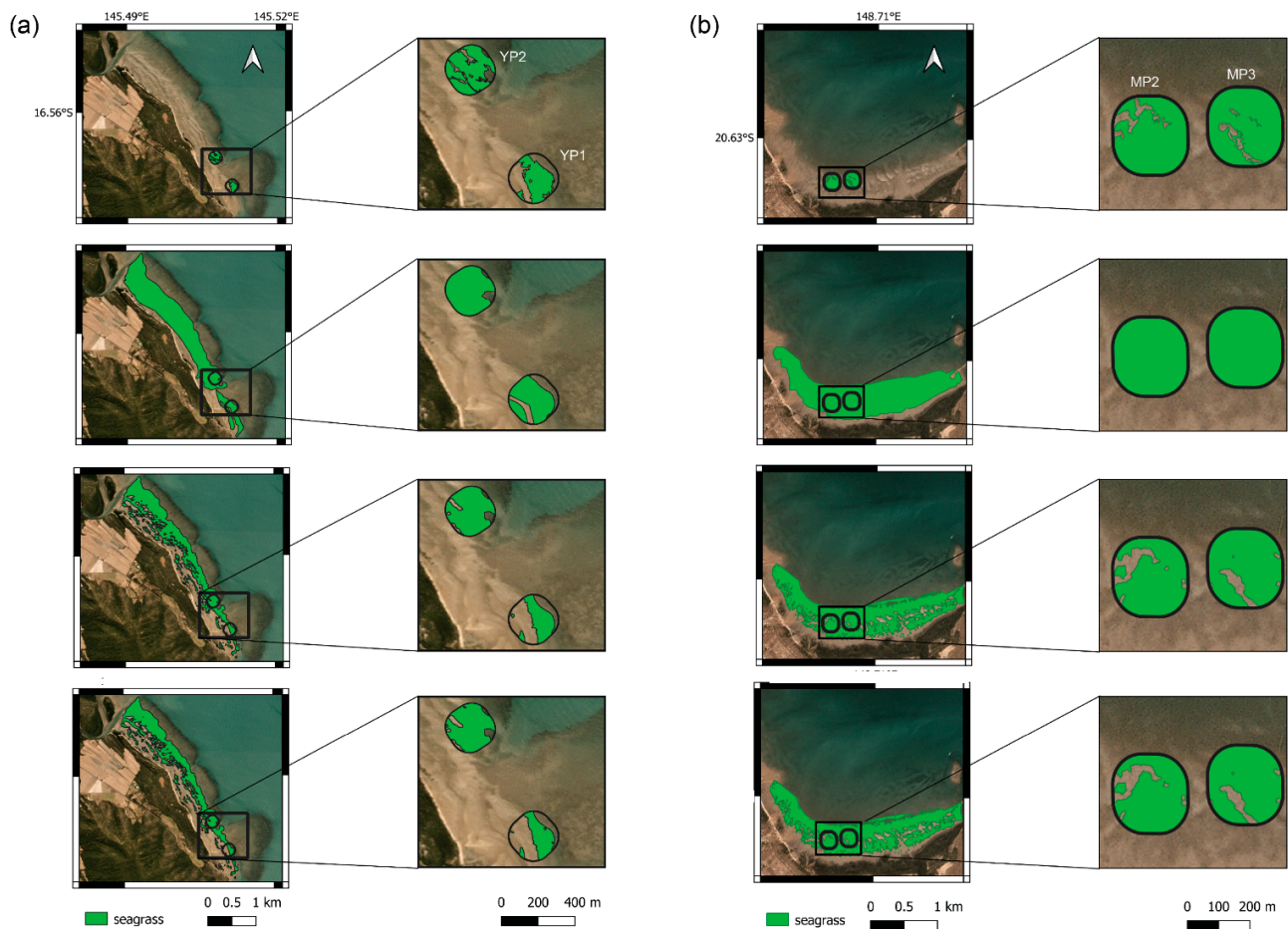


**Figure 8.** Comparison of traditional (in situ by foot and high earth by helicopter) and enhanced (spaceborne) approaches to mapping extent of coastal seagrass communities at meso- and fine-scales in 2017 within the GBRWHA: (a) coastal clear water *Halodule uninervis* with *Halophila ovalis* meadows at Yule Point in 2017; (b) coastal turbid water *Zostera muelleri* meadows at Midge Point in 2017. Left column is meso-scale across banks, and right column is fine-scales within sites. From top: row 1, direct in situ by foot; row 2, high earth by helicopter; row 3, spaceborne by satellite, showing 100% bootstrap probability; and bottom row, spaceborne by satellite, showing 60% bootstrap probability.

### 3.3. Applied Assessment of Enhanced Mapping Approaches

To assess possible improvements in mapping seagrass extent and abundance (in diverse seagrass communities and habitats) using emerging technologies, we focussed on remote sensing approaches using near-field (e.g., UAV) and spaceborne (e.g., satellite) observing platforms.

Using machine-learning technologies, we successfully mapped seagrass abundance classes from the spaceborne-captured imagery in optically clear shallow waters in both coastal and reef habitats (Figures 9 and 10) with an average model accuracy of  $93.67 \pm 0.01$  and  $94.70 \pm 0.01$ , respectively (Table S3). The area of seagrass for each abundance class was calculated at each level of probability, and the respective areas for probabilities between 90 and 60% were relatively similar (Table 7), indicating that the most conservative values representing mapping accuracy would be the bootstrap probabilities of 60 and 100% (Figure 10).

**Table 7.** Area of seagrass abundance classes (hectares) mapped within each AOI at reef and coastal clear water habitats using imagery captured with satellite (PlanetScope) and UAV. BP = bootstrap probability, \* = below bootstrap probability (bBP). AOI for meso-scale spaceborne-captured imagery can differ due to kernelling at the margins of the AOI. n.a. = not assessed. NB: reef clear water meadow covers entire AOI, with no meadow boundary mapped by foot.

AOI	Earth Observing Platform	Map Figure	Area (ha)	BP	Seagrass Abundance Class				Rubble/Algae or bBP	Total Seagrass Area
					Absent	Low	Medium	High		
Coastal clear water (Yule Pt)	by foot	Figure 9b(ii)	0.8020	n.a.	n.a.	n.a.	n.a.	n.a.	n.a.	0.7053
	UAV	Figure 9b(iv)	0.8020	n.a.	0.1192	0.4854	n.a.	0.1701	0.0273	0.6555
	satellite (meso-scale)	Figure 9a(ii)	49.65	100%	22.71	15.60	n.a.	5.18	6.21 *	20.78
			49.65	90%	24.45	17.46	n.a.	5.86	1.95 *	23.32
			49.65	80%	24.90	18.02	n.a.	6.08	0.71 *	24.09
	Figure 9a(i)	49.65	60%	25.12	18.36	n.a.	6.21	0.03 *	24.57	
Reef clear water (Green Is)	UAV	Figure 10f	4.512	n.a.	0	2.193	0.429	1.887	0	4.512
	satellite (fine-scale)	Figure 10d	4.512	100%	0	0.071	2.594	1.685	0.162	4.512
		Figure 10c	4.512	60%	0	0.072	2.695	1.745	0	4.512
	satellite (meso-scale)	Figure 10b	316.62	100%	79.13	26.59	71.49	63.25	32.17 *	316.75
			316.66	90%	82.8	31.09	80.12	66.05	6.7 *	316.82
316.73			80%	83.24	32.17	81.48	66.57	2.07 *	316.89	
	Figure 10a	316.86	60%	83.45	32.89	81.92	66.67	0.08 *	316.99	

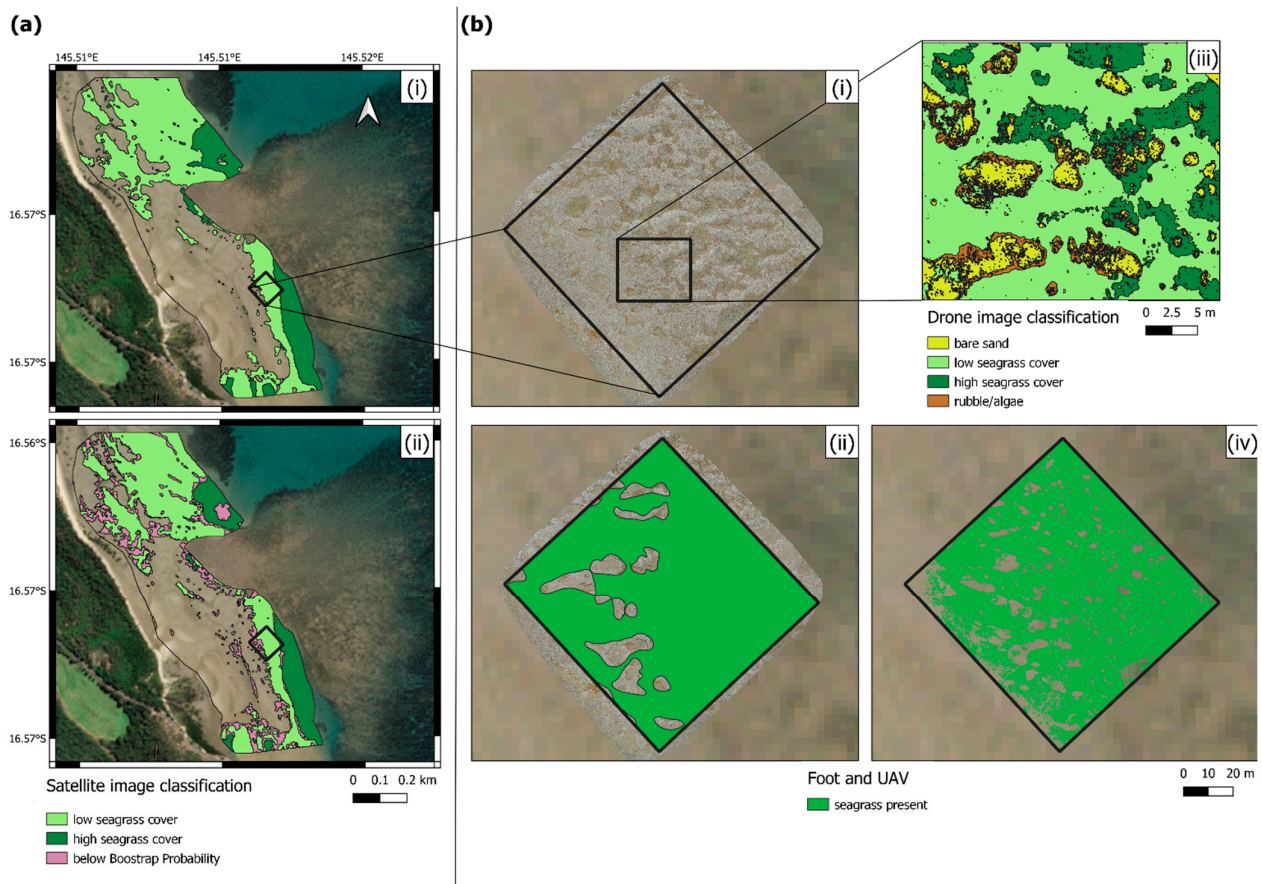


**Figure 9.** Machine- and deep-learning approaches to meso- and fine-scale mapping of seagrass abundance classes in a coastal clear water habitat (Yule Point) in 2019–2020: (a) meso-scale map from spaceborne-captured imagery showing seagrass abundance classes with (i) bootstrap probability of 60% and (ii) 100%; (b) fine-scale maps showing (i) UAV-captured image of AOI; (ii) presence of seagrass mapped in situ by foot; (iii) abundance classes of seagrass mapped using deep-learning; (iv) presence of seagrass mapped using deep-learning, within highlighted section of AOI.

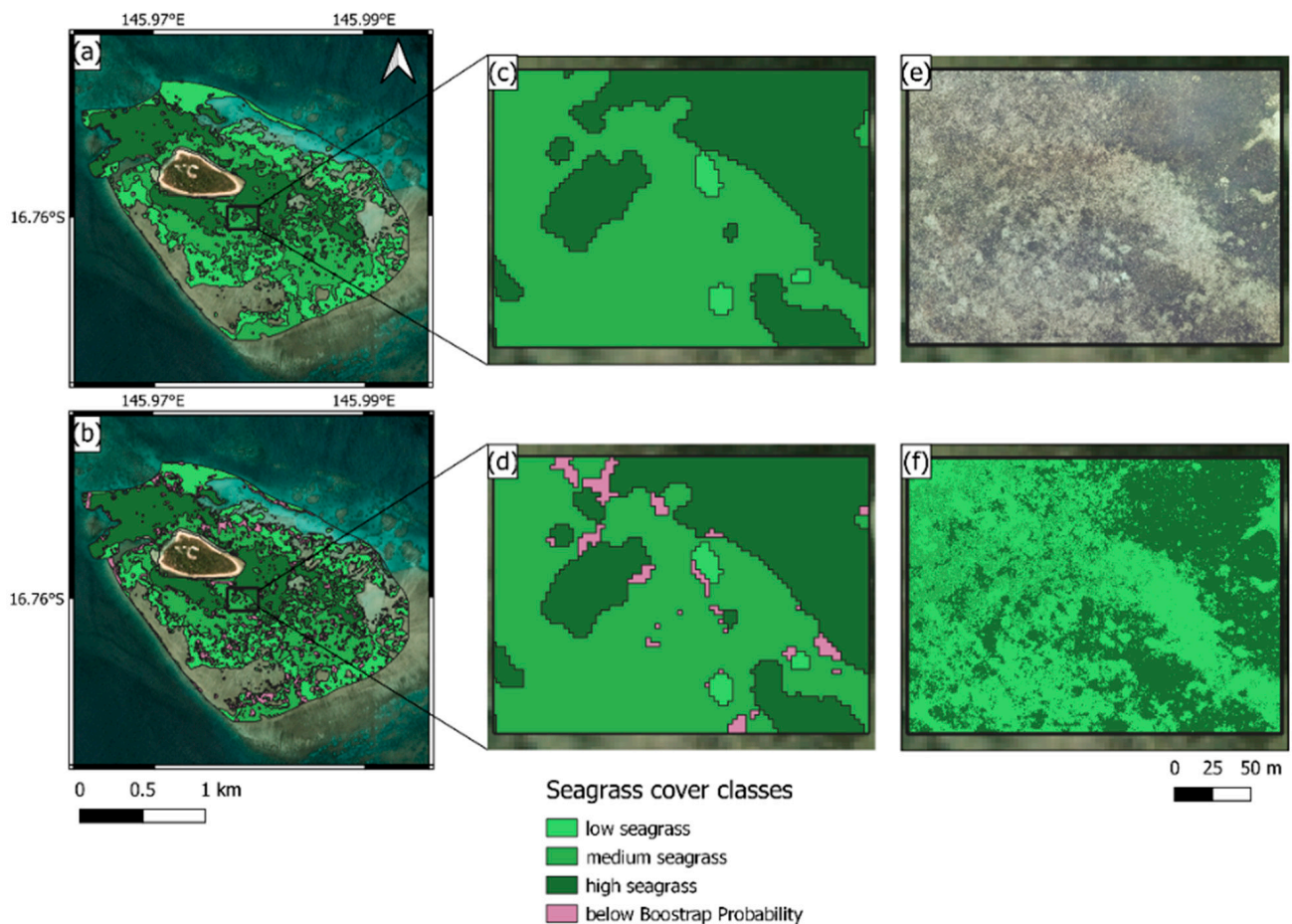


**Figure 10.** Machine- and deep-learning approaches to fine-scale mapping of seagrass abundance classes in an intertidal/shallow subtidal reef habitat, Green Island, in 2020: (a) abundance classes of seagrass mapped with bootstrap probability of 60%, from spaceborne-captured imagery using machine-learning; (b) abundance classes of seagrass mapped with bootstrap probability of 100%, from spaceborne-captured imagery using machine-learning; (c) highlighted AOI showing detail of machine-learning derived map with bootstrap probability of 60%; (d) highlighted AOI showing detail of machine-learning derived map with bootstrap probability of 100%; (e) highlighted AOI showing the UAV-captured imagery; (f) highlighted AOI showing abundance classes of seagrass mapped with deep-learning from UAV-captured imagery.

Using trained deep-learning models (Figures S5 and S6), we successfully mapped the area of seagrass and each abundance class from the UAV-captured imagery within each of the AOIs (Figures 9 and 10). The accuracy of the deep-learning model (represented by the intersection-over-union (IoU) score) was 0.78 and 0.74 for the coastal and reef clear water seagrass habitats, respectively. The UAV-captured imagery had a higher ability to differentiate low and medium abundance classes than the satellite imagery (Table 7). The resolution and resulting meadow-scapes mapped from UAV-captured imagery were also significantly greater and more detailed than could be differentiated using spaceborne-captured imagery or by foot (Figure 10).

#### 4. Discussion

In this study, we completed the most comprehensive systematic review of seagrass mapping conducted within the GBRWHA to date, as well as presented several innovative approaches using machine- and deep-learning to produce seagrass maps of high to very high confidence at fine- and meso-scales from airborne and spaceborne imagery.

#### 4.1. Traditional Mapping Approaches

Although there have been several previous spatial data compilations for the GBRWHA (e.g., [60]), the most detailed from 1984 to 2018 included less than half of the mapping events identified in our assessment for the same period [8]. When conducting our assessment, a key challenge was developing and defining a standardised terminology. We found substantial irregularities in the technical language used in relation to earth observing elements (platforms and types), mapping approach, scale, resolution, and seagrass meadow organisational level. Careful examination of mapping events in the PRISMA eligibility stage (Figure S1) identified instances where authors reported mapping meadows which did not exist. For example, authors conducting “meadow-scale” monitoring theoretically mapped meadows and reported the extent as zero, rather than surveying for seagrass within a defined area and reporting seagrass as absent. The development of a comprehensive glossary of globally standardised terminologies applicable to seagrass ecosystems, mapping, and assessment would benefit future data syntheses both within the GBRWHA and globally.

Our review of mapping events within the GBRWHA highlighted geographic, temporal, and habitat biases. Geographic biases were predominately a consequence of data needs in areas of greatest risk from human activities, e.g., ports [61]. Temporal biases were a consequence of tropical seagrass seasonal growth: to capture seagrass extent when at its annual peak. This was particularly important for annual seagrass species that complete their lifecycle in a single growing season. For example, deep-water *Halophila tricostata* may only persist as a seed bank through the cooler months of the year when light conditions are less favourable [62–64].

We found that the most commonly used mapping approach for intertidal meadows within the GBRWHA was field-based, where GPS tracks and spot-checks captured from helicopters were used to draw boundaries and define meadow characteristics (e.g., species composition, cover, and type of meadow). The resulting products were meso-scale maps of moderate confidence and fine-scale maps of very poor confidence; overestimating the area of seagrass by 6 to 80%, due to the lack of meadowscape measures beyond narrative (e.g., description of continuous, aggregated patches, or isolated patches). We have shown that such approaches could be significantly improved by coupling spot-checks with spaceborne imagery, to produce maps of high confidence.

#### 4.2. Improving Machine- and Deep-Learning Approaches for Seagrass Mapping

Using a machine-learning pixel-based (PB) classification coupled with a bootstrapping process, we were able to significantly improve mapping of seagrass meadows particularly in low density (cover), fragmented, and complex substrate habitats for our case study areas. The resulting probabilities from the bootstrapping process not only provided more accurate measures of seagrass meadow spatial extent, but the inclusion of meadowscape configuration was a significant improvement.

Traditionally, high earth or earth observing from space has been used for land cover classification, using a PB analysis approach. However, when attempting per-pixel classification for the purposes of mapping land classes such as vegetation cover types at a subregional to broad scale, spectral heterogeneity can result in a large number of misclassified pixels appearing within classes, creating a ‘salt and pepper’ effect [65]. Consequently, there has been a recent shift towards an object-based image analysis (OBIA) approach which uses the spectral and spatial properties of groups of pixels that make up segments and divide the image into objects. OBIA classification techniques have been particularly successful for mapping meadows of structurally large seagrass species in coastal and clear water environments [66–70], making mapping possible for submerged meadows. However, those techniques do not appear well-suited for intertidal meadows with lower abundance, structurally smaller species and highly diverse communities and habitats within the GBRWHA. Additionally, the high turbidity of the coastal waters of the GBRWHA restricts the capture of high and moderate spatial resolution imagery to when the meadows are exposed during low spring tides to be suitable for mapping. All these settings may explain why,

to date, less than 1% of all seagrass mapping events within the GBRWHA, excluding the present study, have been conducted using air- and spaceborne imagery.

While there are significant advantages to using the OBIA approach, we found that it was not well-adapted to the seagrass meadow classification we attempted for our case studies. The main factor was that these meadows were highly heterogeneous on account of high levels of fragmentation. Therefore, when OBIA was tested, it resulted in an over-simplification of the seagrass meadowscape which resulted in either over or under predicting the seagrass area. Consequently, we decided to use a PB classification which led to greater resolution and more accurate results, in particular accounting for meadowscape configuration.

To the best of our knowledge, our study was also the first to use deep-learning models to derive seagrass maps from high earth UAV imagery. UAVs, commonly referred to as drones, are becoming popular platforms for spatial assessment of ecological phenomena [71–74], effectively bridging the gap between satellite and onground data collection [75]. These high earth observing platforms have the capacity for acquiring remotely sensed imagery of very fine spatial resolution (0.01–5 cm), have increased flexibility for image acquisition, and generally have lower operational costs. So far, OBIA with machine-learning techniques has been the most commonly used method to derive maps from UAV imagery [76–78]. Deep-learning techniques such as convolutional neural networks (CNN) have emerged as a new effective approach that can identify seagrass [79,80] or specific features such as dugong feeding trails [81], but until now, had not been applied for operational mapping. Here, we used the semantic segmentation technique, which had been previously used for seagrass coverage estimation in underwater photoquadrats [82], and demonstrated its promising potential for fine-scale seagrass mapping. Indeed, coupled with very high-resolution UAV imagery, deep-learning allows for the rapid and highly accurate production of maps to be used to assess important metrics such as meadowscape (e.g., fragmentation).

#### *4.3. Improving Accuracy and Confidence of Maps for Users*

We recognized there appears to be some confusion by map users regarding the confidence in the final map product. Measures of accuracy can often be confusing, as they can relate to different elements of a map, and not the final product. For example, the boundary accuracy [45] is a subjective measure estimated by the map creator, based predominately on the accuracy of the GPS, the spatial extent per observation and the mapping approach. However, this does not account for the size of the AOI relative to the field validation (i.e., representativeness) or the interpolation method employed (i.e., directness). Similarly, the use of a confusion matrix on its own for the assessment of seagrass cover classification accuracy, is insufficient to represent the confidence of the final map as it does not account for representativeness of the AOI or the extent of the field validation. Throughout the process of the writing of this study, it became clear that careful appraisal of the final map output is crucial. The appraisal should aim to assess if the final map product is plausible and based on multiple lines of evidence, such as expert knowledge of seagrass physiology and growth requirements and marine benthic ecology or historical knowledge of the AOI. The outcome of the appraisal can be used as a feedback loop to rectify errors and rerun the process (i.e., components of the workflow) if needed, until optimal results are reached.

Another major source of potential bias and error for the remote sensing techniques occurs when matching in situ validation data to georectified imagery. For example, when using photoquadrats (0.25–1.0 m<sup>2</sup> area) that are geotagged (geospatial information captured in the metadata) or geolocated using a handheld GPS (i.e., points), map creators must acknowledge a spatial positioning error of 1.5 to 3 m for the point. When aligning a point to satellite-captured imagery of 3 m pixel resolution, it is possible for a point to potentially match with at least 9 pixels which represent an area of 9 m<sup>2</sup>. If that seagrass area is heterogeneous and the photoquadrat not representative of the overall 9 m<sup>2</sup>, this can lead to conflicting training information for the machine-learning model and ultimately

an unreliable output. Therefore, field validation data design is paramount and needs to be thoroughly revealed and explained alongside the results to ensure validity and confidence in the mapping product. Furthermore, as technology progresses, access to real-time kinematic positioning (RTK) UAVs will be more affordable and may alleviate these issues.

#### 4.4. Improving Field Data Capture

As the intertidal areas of the GBRWHA extend over 2500 km of coastline, helicopters have been the most cost-efficient observing platform for conducting in situ field validation (spot-check measures) in remote regions. During seagrass mapping, a field spot-check generally includes recording single or replicate measures (e.g., three 0.25 m<sup>2</sup> quadrats) at a point (10 m<sup>2</sup>) to capture seagrass variance. These spot-checks have traditionally only been conducted by human observation but could be greatly improved by migrating to geotagged photoquadrats, e.g., GoPro cameras mounted to the helicopter skid crossbar for nadir image capture. However, using helicopters as the observing platform does not come without challenges. Of concern is downdraft, which obscures observations, and greenhouse gas emissions; helicopters used for mapping emit 60 to 100 kg CO<sub>2</sub> h<sup>-1</sup> [83]. An alternative is UAVs, which provide an excellent observing platform for capture of both orthophotos and in situ spot-checks, particularly where meadows can be examined within visual line-of-sight of the operator; up to approximately 500 m radius [84]. A UAV at 3 m altitude can capture a standardised nadir image covering an area of approximately 3 × 4.5 m. By classifying three or more random nonoverlapping pixel-clusters (equivalent to the size of a 0.25 m<sup>2</sup> quadrat) within each UAV-captured image and taking the average would ensure capture of seagrass heterogeneity. An optimal flight plan would enable spot-checks to sufficiently cover large intertidal areas using a UAV. For orthophotos, larger areas can be assessed in fine detail by multiple operators simultaneously mapping a grid design using small UAVs [85]. Alternatively, larger UAVs can be operated beyond visual line-of-sight (BVLOS); however, this requires a remote pilot licence (RePL). We envision at some time in the future, when battery technologies enable extended flight times, that squadrons of both small and large BVLOS UAVs can be tasked to capture higher altitude orthophotos and/or conduct low altitude spot-checks/phototranssects for validating imagery and mapping the intertidal and clear shallow water seagrasses of the entire GBRWHA within a single austral growing season.

#### 4.5. Improving Mapping for Policy and Management Decisions

We considered that the use of the confidence scoring using defined categories provides a more transparent process and understanding of a seagrass map for users. Users are predominately environmental practitioners and managers, who use the maps as evidence upon which policy and management decisions can be made. Our study demonstrated that emerging technologies and enhanced analysis techniques can greatly improve the accuracy and confidence in the final mapping product. These improvements are not only applicable to future seagrass mapping events but may afford improvements to previous mapping. For example, we re-examined a mapping event conducted in 2001 which used traditional approaches (e.g., helicopter) [86], and found, using the original spot-check data and aerial imagery, that the area of seagrass was approximately half what was originally reported (Figure S7, Table S4). This was primarily a consequence of the original mapping not accounting for meadowscape within the measure of area. The use of a narrative to describe meadowscape is generally lost on a map user, as it is not clear how it should be interpreted or used, particularly when assessing change over time. Until the inclusion of meadowscape measures is routine, we recommend the incorporation of a correction factor depending on the level of meadow fragmentation. A key priority will be to educate marine environment managers on how to interpret the confidence and meadowscape measures.

Our improved approaches not only provide users/environmental managers with more accurate measures of seagrass meadow spatial extent, but the inclusion of meadowscape

configuration enables enhanced measures of seagrass ecosystem goods and benefits. For example, in blue carbon accounting, measures should factor for the effects of meadowscape when estimating seagrass blue carbon stocks, as a large, continuous meadow stores more blue carbon than an equal area of small patches [87–89]. To account for this, it is recommended that the area of a meadow within the first 10 m from an edge should be excluded to avoid overestimation [89]. When applying this consideration to our meso-scale mapping exercises, the estimation of carbon stocks from maps constructed using the traditional high earth observing method (e.g., helicopter, which does not include meadowscape measures) were almost double that of the estimation produced from our improved spaceborne method, which included greater meadowscape detail.

#### 4.6. Improving Mapping Using Habitat Suitability Modelling

In the last decade, modelling approaches have shown some promise; however, the underlying data remains limited and spatially biased. Carter et al. [90] identified 88,331 km<sup>2</sup> of potential seagrass habitat in intertidal and subtidal areas of the GBRWHA using random forest and multivariate regression tree models to assign seagrass probability ( $\geq 0.2$ ) and community type (36 identified) to individual pixels (900 m<sup>2</sup>). However, as we showed in our current analysis, existing GBRWHA mapping data which underlies the potential seagrass habitat model [90] is heavily spatially biased and predominately focussed on locations where seagrass are known or suspected to occur, which can compromise model performance [91]. As a consequence, this type of modelling approach could be improved if field data that drives the model is more representative, particularly for locations where the absence of seagrass is underrepresented [10]. For example, shallow subtidal habitats on coral reefs have been poorly assessed across the GBRWHA, as these habitats are either colonised by coral and/or predominately consolidated sediments, which are unlikely to provide suitable habitat for seagrass colonisation (with the exception of *Thalassodendron ciliatum*). Shallow subtidal reef habitats are also poorly represented in the existing sediment databases (which are modelled), and the reef geomorphology database is outdated [24]. To improve the potential seagrass habitat model (particularly for underrepresented habitats), additional lines of evidence should be included, such as data capture from citizen science, traditional ecological knowledge, and the coupling of spot-checks with airborne and/or spaceborne imagery in optically clear waters.

#### 4.7. Improving Mapping for Deeper Subtidal Habitats

Although our study focussed on intertidal and shallow subtidal meadows in mostly optically clear waters, we believe the approaches currently used to map subtidal seagrasses in deep (>10 m) and optically complex waters can similarly be improved. At the elemental level, these improvements include increasing the quantity and spread of field validation points, including direct visual spot-checks, photoquadrats, or samplers (e.g., grab). As new technologies emerge, we will see improved methods for data/image capture and analysis, and positional accuracy. Continuous improvements in AI and deep-learning technologies will expedite analysis of imagery for seagrass occurrence, abundance, and species forms/characteristics. Much like UAVs, autonomous underwater vehicles (AUVs) are rapidly advancing with extended deployment times and improved sensors for image capture and analysis. Soon, AUVs will be able to swath map large areas of the seabed, and when coupled with increased positional accuracy, will provide orthomosaics which can be used to produce spatially explicit maps of high confidence. In preparation for such developments, we are currently researching deep-learning models to provide a subtidal seagrass detector to optimise routine analysis of the captured imagery.

#### 4.8. Improving Mapping through Increased Collaboration

Finally, mapping seagrasses in the optically complex and deep waters of the GBRWHA can be greatly improved by accessing field data gathered by a broader range of providers, including stakeholders, industry, traditional owners (First Nations peoples) and citizen

scientists, i.e., big data [92]. Although big data can be difficult to analyse/manage with traditional means, as the data sets are so large and collected so rapidly, continued advances in deep-learning techniques and increased access to high end and cloud computing will enable the mainstreaming of big data for routine assessments of large study areas such as the GBRWHA. This will build on initiatives such as SeagrassSpotter, where users contribute geotagged photos via a smartphone app, which provides invaluable in situ spot-check data for mapping validation and citizen engagement [93]. Support for continued development of technologies is key, but this will also require improved outreach and engagement, highlighting the benefits of increased collaboration.

#### 4.9. Recommendations for Future Seagrass Mapping Events in the GBRWHA

- Ensure routine collection of geolocated/geotagged photoquadrats to support new and repeated field data collection for training and validation, and provide ability to revisit images for alternate analysis over time;
- Prioritise airborne or spaceborne imagery for seagrass mapping of those environments where seagrass features can be differentiated, such as intertidal and shallow subtidal habitats;
- Transition to UAVs and all-electric observing platforms to improve capture of high-resolution imagery while also reducing greenhouse emissions;
- Maximise use of low altitude and high-resolution image capture (e.g., UAVs) to provide in situ field validation (e.g., spot-checks) where possible;
- Operationalise the routine inclusion of meadowscape metrics in all seagrass maps,
- Ensure all maps of seagrass meadow spatial extent include a measure of confidence, determined using a clear process where all key measures of accuracy, precision, and resolution are transparent to the map user;
- Ensure habitat suitability models for seagrasses are based on comprehensive data and include multiple lines of evidence, such as expert knowledge and coupling with remotely sensed imagery;
- Encourage participatory seagrass mapping, including in situ field validation data, with First Nations peoples and citizen scientists to provide big data solutions.

## 5. Conclusions

In this paper, we completed the most comprehensive systematic review of seagrass mapping conducted within the GBRWHA to date. We demonstrated how existing approaches to map seagrass meadows in intertidal and shallow optically complex waters can be improved using new and emerging technologies. We used case studies to harness the power of machine- and deep-learning for seagrass cover mapping with PlanetScope and UAV-captured imagery in three very different settings: coastal clear and turbid water, and reef clear water habitats of the Great Barrier Reef. Using a machine-learning pixel-based classification coupled with a bootstrapping process, we were able to significantly improve maps of seagrass meadows, particularly in low density (cover), fragmented, and complex substrate habitats. To the best of our knowledge, our study was also the first to use deep-learning models to derive maps from high earth UAV imagery. To better inform map users, we also proposed a multicriteria approach to semiquantitatively score the confidence of a mapping product. Overall, these improvements are applicable not only for ongoing, routine monitoring and time series analysis at fine- and meso-scales, but to GBR-wide and potentially global extents.

**Supplementary Materials:** The following are available online at <https://www.mdpi.com/article/10.3390/rs14112604/s1>, Table S1: Seagrass mapping events in the GBRWHA, Table S2: Map confidence evaluation criteria [37], Table S3: Summary of machine-learning model outputs, Table S4: Cairns Harbour seagrass area comparison, Figure S1: PRISMA [35] flow diagram, Figure S2: Validation points and segments for coastal AOIs 2017, Figure S3: Validation points and segments for coastal AOIs 2019, Figure S4: Validation points and segments for reef AOIs 2020, Figure S5: Deep-learning output from coastal UAV 2019, Figure S6: Deep-learning output from reef UAV 2020, Figure S7:

Cairns Harbour mapping approaches comparison [86,94]. Section S3: Additional machine- and deep-learning methods and results [95,96].

**Author Contributions:** Conceptualisation, L.J.M. and L.A.L.; methodology, L.J.M. and L.A.L.; validation, L.J.M. and L.A.L.; formal analysis, L.J.M. and L.A.L.; investigation, L.J.M. and L.A.L.; resources, L.J.M.; data curation, L.A.L.; writing—original draft preparation, L.J.M., L.A.L., and C.M.R.; writing—review and editing, L.J.M., L.A.L. and C.M.R.; visualisation, L.J.M., L.A.L. and C.M.R. All authors have read and agreed to the published version of the manuscript.

**Funding:** The field component of this research was partially funded by the Commonwealth of Australia, acting through the Great Barrier Reef Marine Park Authority (GBRMPA) for the Marine Monitoring Program.

**Data Availability Statement:** UAV orthomosaics are available at <https://data.geonadir.com/> (accessed on 8 May 2022). The seagrass maps generated from this study are available from Pangaea.de (<https://doi.org/TBA>). The R code is available on request from L.J.M. and L.A.L.

**Acknowledgments:** We thank Rudi Yoshida, Haley Brien, Abby Fatland, Jasmina Uusitalo, Naomi Smith, Louise Johns, and Catherine Collier for assistance with data collection. We thank Christina Howley (Howley Environmental Consulting) and Carol Conacher (frc environmental) for their assistance locating and providing consultancy reports of mapping events. We also thank Katherine Martin, Bronwyn Houlden, and Carol Honchin from the GBRMPA for their support through the Marine Monitoring Program. PlanetScope ortho scene satellite imagery was acquired courtesy of the Planet Education and Research program. We also thank the Traditional Owners of the sea countries we visited to conduct our research: Yirrganydji, Guru-Gulu Gunggandji, and Gia.

**Conflicts of Interest:** The authors declare no conflict of interest.

## References

- Joyce, R.B. Time and Captain Cook. *Queensland Heritage* **1970**, *2*, 8–12.
- Cook, J.; Hutchinson, J.; Wallis, S.; Bolckow, H.W.F. Journal of HMS Endeavour, Lieutenant James Cook, Commander, from May 1768 to July 1771. 1768. Available online: <http://nla.gov.au/nla.obj-228958440> (accessed on 26 April 2021).
- Kuo, J.; Cambridge, M.L.; McKenzie, L.J.; Coles, R.G. Taxonomy of Australian Seagrasses. In *Seagrasses of Australia: Structure, Ecology and Conservation*; Larkum, A.W.D., Kendrick, G.A., Ralph, P.J., Eds.; Springer International Publishing: Cham, Switzerland, 2018; pp. 759–782. [\[CrossRef\]](#)
- Brown, R. Monocotyledones. In *Prodromus Florae Novae Hollandiae et Insulae Van-Diemen: Exhibens Characteres Plantarum Quas Annis 1802–1805 per Oras Utriusque Insulae Collegit et Descripsit Robertus Brown; Insertis Passim Aliis Speciebus Auctori Hucusque Cognitis, seu Evulgatis, seu Ineditis, Praesertim Banksianis, in Primo Itinere Navarchi Cook Detectis*; J. Johnson et Socios: Londini, UK, 1810; Volume 1, pp. 145–590.
- Coles, R.G.; Rasheed, M.A.; McKenzie, L.J.; Grech, A.; York, P.H.; Sheaves, M.; McKenna, S.; Bryant, C. The Great Barrier Reef World Heritage Area seagrasses: Managing this iconic Australian ecosystem resource for the future. *Estuar. Coast. Shelf Sci.* **2015**, *153*, A1–A12. [\[CrossRef\]](#)
- Marsh, H.; Saalfeld, W.K. The distribution and abundance of dugongs in the Northern Great Barrier Reef Marine Park. *Aust. Wildl. Res.* **1989**, *16*, 429–440. [\[CrossRef\]](#)
- McKenzie, L.J.; Yoshida, R.L.; Grech, A.; Coles, R. Composite of coastal seagrass meadows in Queensland, Australia November 1984 to June 2010. *Pangaea* **2014**. [\[CrossRef\]](#)
- Carter, A.B.; McKenna, S.A.; Rasheed, M.A.; Collier, C.; McKenzie, L.; Pitcher, R.; Coles, R. Synthesizing 35 years of seagrass spatial data from the Great Barrier Reef World Heritage Area, Queensland, Australia. *Limnol. Oceanogr. Lett.* **2021**, *6*, 216–226. [\[CrossRef\]](#)
- GBRMPA. *Great Barrier Reef Features*; Great Barrier Reef Marine Park Authority: Townsville, Australia, 2014. Available online: <http://www.gbrmpa.gov.au/geoportals/> (accessed on 26 June 2021).
- McKenzie, L.J.; Nordlund, L.M.; Jones, B.L.; Cullen-Unsworth, L.C.; Roelfsema, C.; Unsworth, R.K. The global distribution of seagrass meadows. *Environ. Res. Lett.* **2020**, *15*, 074041. [\[CrossRef\]](#)
- Gacia, E.; Duarte, C.M.; Marba, N.; Terrados, J.; Kennedy, H.; Fortes, M.D.; Tri, N.H. Sediment deposition and production in SE-Asia seagrass meadows. *Estuar. Coast. Shelf Sci.* **2003**, *56*, 909–919. [\[CrossRef\]](#)
- Lamb, J.B.; van de Water, J.A.J.M.; Bourne, D.G.; Altier, C.; Hein, M.Y.; Fiorenza, E.A.; Abu, N.; Jompa, J.; Harvell, C.D. Seagrass ecosystems reduce exposure to bacterial pathogens of humans, fishes, and invertebrates. *Science* **2017**, *355*, 731–733. [\[CrossRef\]](#)
- Madsen, J.D.; Chambers, P.A.; James, W.F.; Koch, E.W.; Westlake, D.F. The interaction between water movement, sediment dynamics and submersed macrophytes. *Hydrobiologia* **2001**, *444*, 71–84. [\[CrossRef\]](#)
- Marsh, H.; O’Shea, T.J.; Reynolds, J.E., III. *Ecology and Conservation of the Sirenia*; Cambridge University Press: Cambridge, UK, 2011.

15. Esteban, N.; Mortimer, J.A.; Stokes, H.J.; Laloë, J.-O.; Unsworth, R.K.F.; Hays, G.C. A global review of green turtle diet: Sea surface temperature as a potential driver of omnivory levels. *Mar. Biol.* **2020**, *167*, 183. [[CrossRef](#)]
16. Duarte, C.M.; Krause-Jensen, D. Export from Seagrass Meadows Contributes to Marine Carbon Sequestration. *Front. Mar. Sci.* **2017**, *4*, 13. [[CrossRef](#)]
17. Fourqurean, J.W.; Duarte, C.M.; Kennedy, H.; Marba, N.; Holmer, M.; Mateo, M.A.; Apostolaki, E.T.; Kendrick, G.A.; Krause-Jensen, D.; McGlathery, K.J.; et al. Seagrass ecosystems as a globally significant carbon stock. *Nat. Geosci.* **2012**, *5*, 505–509. [[CrossRef](#)]
18. Unsworth, R.K.F.; Collier, C.J.; Henderson, G.M.; McKenzie, L.J. Tropical seagrass meadows modify seawater carbon chemistry: Implications for coral reefs impacted by ocean acidification. *Environ. Res. Lett.* **2012**, *7*, 024026. [[CrossRef](#)]
19. Cullen-Unsworth, L.; Unsworth, R. Seagrass Meadows, Ecosystem Services, and Sustainability. *Environ. Sci. Policy Sustain. Dev.* **2013**, *55*, 14–28. [[CrossRef](#)]
20. Unsworth, R.K.F.; McKenzie, L.J.; Collier, C.J.; Cullen-Unsworth, L.C.; Duarte, C.M.; Eklöf, J.S.; Jarvis, J.C.; Jones, B.L.; Nordlund, L.M. Global challenges for seagrass conservation. *Ambio* **2019**, *48*, 801–815. [[CrossRef](#)]
21. McKenzie, L.J.; Collier, C.J.; Langlois, L.A.; Yoshida, R.L.; Uusitalo, J.; Waycott, M. *Marine Monitoring Program: Annual Report for Inshore Seagrass Monitoring 2019–2020. Report for the Great Barrier Reef Marine Park Authority*; Great Barrier Reef Marine Park Authority: Townsville, Australia, 2021; p. 168.
22. O'Brien, K.R.; Waycott, M.; Maxwell, P.; Kendrick, G.A.; Udy, J.W.; Ferguson, A.J.P.; Kilminster, K.; Scanes, P.; McKenzie, L.J.; McMahon, K.; et al. Seagrass ecosystem trajectory depends on the relative timescales of resistance, recovery and disturbance. *Mar. Pollut. Bull.* **2018**, *134*, 166–176. [[CrossRef](#)]
23. Kilminster, K.; McMahon, K.; Waycott, M.; Kendrick, G.A.; Scanes, P.; McKenzie, L.; O'Brien, K.R.; Lyons, M.; Ferguson, A.; Maxwell, P.; et al. Unravelling complexity in seagrass systems for management: Australia as a microcosm. *Sci. Total Environ.* **2015**, *534*, 97–109. [[CrossRef](#)]
24. Roelfsema, C.M.; Lyons, M.B.; Castro-Sanguino, C.; Kovacs, E.M.; Callaghan, D.; Wettle, M.; Markey, K.; Borrego-Acevedo, R.; Tudman, P.; Roe, M.; et al. How Much Shallow Coral Habitat Is There on the Great Barrier Reef? *Remote Sens.* **2021**, *13*, 4343. [[CrossRef](#)]
25. Udy, J.; Waycott, M.; Collier, C.; Kilminster, K.; McMahon, K.; Rasheed, M.; MCKENZIE, L.J.; Carter, A.; Lawrence, E.; Maxwell, P.; et al. *Monitoring seagrass within the Reef 2050 Integrated Monitoring and Reporting Program*; Great Barrier Reef Marine Park Authority: Townsville, Australia, 2018; p. 94.
26. Carter, A.B.; McKenna, S.A.; Rasheed, M.A.; McKenzie, L.J.; Coles, R.G. *Seagrass Mapping Synthesis: A Resource for Coastal Management in the Great Barrier Reef World Heritage Area. Report to the National Environmental Science Programme*; Reef and Rainforest Research Centre Limited: Cairns, Australia, 2016; p. 22.
27. Carter, A.B.; McKenna, S.A.; Rasheed, M.A.; McKenzie, L.J.; Coles, R.G. *Collation of Spatial Seagrass Data (Meadow Extent Polygons, Species Presence/Absence Points) from 1984–2014 for the Great Barrier Reef World Heritage Area (GBRWHA) (NESP TWQ 3.1, TropWATER, JCU)*; eAtlas DatasetAIMS: Townsville, Australia, 2016.
28. Derbyshire, K.J.; Willoughby, S.R.; McColl, A.L.; Hocroft, D.M. *Small Prawn Habitat and Recruitment Study: Final Report to the Fisheries Research and Development Corporation and the Queensland Fisheries Management Authority*; Department of Primary Industries: Cairns, Australia, 1995; p. 43.
29. Campbell, S.J.; McKenzie, L.J.; Kerville, S.P.; Bité, J.S. Patterns in tropical seagrass photosynthesis in relation to light, depth and habitat. *Estuar. Coast. Shelf Sci.* **2007**, *73*, 551–562. [[CrossRef](#)]
30. Coles, R.; McKenzie, L.J.; De'ath, G.; Roelofs, A.; Lee Long, W.J. Spatial distribution of deepwater seagrass in the inter-reef lagoon of the Great Barrier Reef World Heritage Area. *Mar. Ecol. Prog. Ser.* **2009**, *392*, 57–68. [[CrossRef](#)]
31. Petus, C.; Devlin, M.; Thompson, A.; McKenzie, L.; Teixeira da Silva, E.; Collier, C.; Tracey, D.; Martin, K. Estimating the Exposure of Coral Reefs and Seagrass Meadows to Land-Sourced Contaminants in River Flood Plumes of the Great Barrier Reef: Validating a Simple Satellite Risk Framework with Environmental Data. *Remote Sens.* **2016**, *8*, 210. [[CrossRef](#)]
32. Carruthers, T.; Dennison, W.; Longstaff, B.; Waycott, M.; Abal, E.G.; McKenzie, L.J.; Lee Long, W. Seagrass habitats of north east Australia: Models of key processes and controls. *Bull. Mar. Sci.* **2002**, *71*, 1153–1169.
33. Grech, A.; Chartrand-Miller, K.; Erfteimeijer, P.; Fonseca, M.; McKenzie, L.J.; Rasheed, M.; Taylor, H.; Coles, R. A comparison of threats, vulnerabilities and management approaches in global seagrass bioregions. *Environ. Res. Lett.* **2012**, *7*, 024006. [[CrossRef](#)]
34. Devlin, M.; Petus, C.; da Silva, E.; Tracey, D.; Wolff, N.; Waterhouse, J.; Brodie, J. Water Quality and River Plume Monitoring in the Great Barrier Reef: An Overview of Methods Based on Ocean Colour Satellite Data. *Remote Sens.* **2015**, *7*, 12909. [[CrossRef](#)]
35. Moher, D.; Liberati, A.; Tetzlaff, J.; Altman, D.G. Preferred reporting items for systematic reviews and meta-analyses: The PRISMA statement. *BMJ* **2009**, *339*, b2535. [[CrossRef](#)]
36. DAF. *Queensland Commercial Fishery 30 Minute Reporting Grid Metadata Record*; Department of Agriculture and Fisheries: Brisbane, QLD, Australia, 2021. Available online: <https://www.data.qld.gov.au/dataset/queensland-commercial-fishery-30-minute-reporting-grid> (accessed on 20 June 2021).
37. Waterhouse, J.; Henry, N.; Mitchell, C.; Smith, R.; Thomson, B.; Carruthers, C.; Bennett, J.; Brodie, J.; McCosker, K.; Northey, A.; et al. *Paddock to Reef Integrated Monitoring, Modelling and Reporting Program, Program design 2018–2022*; Australian and Queensland, Government: Brisbane, Australia, 2018; p. 137.

38. Phinn, S.; Roelfsema, C.; Kovacs, E.; Canto, R.; Lyons, M.; Saunders, M.; Maxwell, P. Mapping, Monitoring and Modelling Seagrass Using Remote Sensing Techniques. In *Seagrasses of Australia*; Larkum, A.W., Ralph, P.J., Kendrick, G.A., Eds.; Springer: Cham, Switzerland, 2018; pp. 445–487.
39. Hossain, M.S.; Hashim, M. Potential of Earth Observation (EO) technologies for seagrass ecosystem service assessments. *Int. J. Appl. Earth Obs. Geoinf.* **2019**, *77*, 15–29. [[CrossRef](#)]
40. Bailey, R.G. The factor of scale in ecosystem mapping. *Environ. Manag.* **1985**, *9*, 271–275. [[CrossRef](#)]
41. Bailey, R.G. Suggested hierarchy of criteria for multi-scale ecosystem mapping. *Landsc. Urban Plan.* **1987**, *14*, 313–319. [[CrossRef](#)]
42. Goodchild, M.F.; Parks, B.O.; Steyaert, L.T. *Environmental Modeling with GIS*; Oxford University Press: New York, NY, USA, 1993.
43. Roelfsema, C.; Kovacs, E.; Ortiz, J.C.; Wolff, N.H.; Callaghan, D.; Wettle, M.; Ronan, M.; Hamylton, S.M.; Mumby, P.J.; Phinn, S. Coral reef habitat mapping: A combination of object-based image analysis and ecological modelling. *Remote Sens. Environ.* **2018**, *208*, 27–41. [[CrossRef](#)]
44. Roelfsema, C.M.; Kovacs, E.M.; Ortiz, J.C.; Callaghan, D.P.; Hock, K.; Mongin, M.; Johansen, K.; Mumby, P.J.; Wettle, M.; Ronan, M.; et al. Habitat maps to enhance monitoring and management of the Great Barrier Reef. *Coral Reefs* **2020**, *39*, 1039–1054. [[CrossRef](#)]
45. McKenzie, L.J.; Finkbeiner, M.A.; Kirkman, H. Methods for mapping seagrass distribution. In *Global Seagrass Research Methods*; Short, F.T., Coles, R.G., Eds.; Elsevier Science B.V.: Amsterdam, The Netherlands, 2001; pp. 101–121. [[CrossRef](#)]
46. McKenzie, L.J.; Collier, C.; Langlois, L.; Yoshida, R.; Smith, N.; Waycott, M. *Reef Rescue Marine Monitoring Program—Inshore Seagrass, Annual Report for the sampling period 1st June 2013–31st May 2014*; TropWATER, James Cook University: Cairns, Australia, 2015; p. 226. Available online: <https://elibrary.gbrmpa.gov.au/jspui/handle/11017/2976> (accessed on 14 March 2022).
47. McKenzie, L.J.; Campbell, S.J.; Roder, C.A. *Seagrass-Watch: Manual for Mapping & Monitoring Seagrass Resources*, 2nd ed.; QFS, NFC: Cairns, Australia, 2003.
48. McKenzie, L.J.; Yoshida, R.L.; Unsworth, R.K.F. Disturbance influences the invasion of a seagrass into an existing meadow. *Mar. Pollut. Bull.* **2014**, *86*, 186–196. [[CrossRef](#)]
49. Environmental Systems Research Institute. *ArcGIS Desktop: Release 10.7*; Environmental Systems Research Institute: Redlands, CA, USA, 2021.
50. Labelbox Labelbox. Available online: <https://labelbox.com> (accessed on 19 May 2022).
51. Planet. *Planet Imagery Product Specifications*; Planet Labs Inc.: San Francisco, CA, USA, 2021; p. 100.
52. Planet Team. *Planet Application Program Interface: In Space for Life on Earth*; Planet Labs Inc.: San Francisco, CA, USA, 2017; Available online: <https://api.planet.com> (accessed on 14 March 2022).
53. R Core Team. *R: A Language and Environment for Statistical Computing*; R Foundation for Statistical Computing: Vienna, Austria, 2021.
54. Wright, M.N.; Ziegler, A. Ranger: A Fast Implementation of Random Forests for High Dimensional Data in C++ and R. *J. Stat. Softw.* **2017**, *77*, 1–17. [[CrossRef](#)]
55. Esri Inc. *ArcGIS Pro (Version 2.5)*; Environmental Systems Research Institute: Redlands, CA, USA, 2021; Available online: <https://www.esri.com/en-us/arcgis/products/arcgis-pro/overview> (accessed on 14 March 2022).
56. Joseph, V.R. Optimal ratio for data splitting. *Stat. Anal. Data Min. ASA Data Sci. J.* **2022**, 1–8. [[CrossRef](#)]
57. Stephenson, T.; Stephenson, A.; Tandy, G. The structure and ecology of Low Isles and other reefs. *Great Barrier Reef Exped. 1928–1929 Sci. Rep.* **1931**, *3*, 17–112.
58. Manton, S.M.; Stephenson, T.A. Ecological surveys of coral reefs. *Sci. Rep./Great Barrier Reef Exped. 1928–1929* **1935**, *3*, 273–312.
59. van R. Classen, D.; Jupp, D.; Bolton, J.J.; Zell, L. *An Initial Investigation into the Mapping of Seagrass and Water Colour with CZCS and Landset in North Queensland, Australia*; Great Barrier Reef Marine Park Authority and CSIRO Division of Water and Land Resources: Townsville, Australia, 1984; p. 19.
60. McKenzie, L.J.; Yoshida, R.L.; Grech, A.; Coles, R. *Queensland seagrasses. Status 2010—Torres Strait and East Coast*; Fisheries Queensland (DEEDI): Cairns, Australia, 2010; p. 6.
61. Rasheed, M.A. *Seagrass Monitoring in Queensland Ports. Program Summary 2013. A Report for Queensland Ports Association (QPA) TropWATER Publication 13/25*; Centre for Tropical Water & Aquatic Ecosystem Research, JCU: Cairns, Australia, 2013; p. 30.
62. Chartrand, K.M.; Szabó, M.; Sinutok, S.; Rasheed, M.A.; Ralph, P.J. Living at the margins—The response of deep-water seagrasses to light and temperature renders them susceptible to acute impacts. *Mar. Environ. Res.* **2018**, *136*, 126–138. [[CrossRef](#)]
63. York, P.H.; Carter, A.B.; Chartrand, K.; Sankey, T.; Wells, L.; Rasheed, M.A. Dynamics of a deep-water seagrass population on the Great Barrier Reef: Annual occurrence and response to a major dredging program. *Sci. Rep.* **2015**, *5*, 13167. [[CrossRef](#)]
64. Kuo, J.; Lee Long, W.J.; Coles, R.G. Occurrence and fruit and seed biology of *Halophila tricostata* Greenway (Hydrocharitaceae). *Aust. J. Mar. Freshw. Res.* **1993**, *44*, 43–57. [[CrossRef](#)]
65. Blaschke, T.; Lang, S.; Lorup, E.; Strobl, J.; Zeil, P. Object-oriented image processing in an integrated GIS/remote sensing environment and perspectives for environmental applications. In *Environmental Information for Planning, Politics and the Public*; Cremers, A., Greve, K., Eds.; Metropolis Verlag: Marburg, Germany, 2000; Volume 2, pp. 555–570.
66. Roelfsema, C.M.; Lyons, M.; Kovacs, E.M.; Maxwell, P.; Saunders, M.I.; Samper-Villarreal, J.; Phinn, S.R. Multi-temporal mapping of seagrass cover, species and biomass: A semi-automated object based image analysis approach. *Remote Sens. Environ.* **2014**, *150*, 172–187. [[CrossRef](#)]

67. Topouzelis, K.; Makri, D.; Stoupas, N.; Papakonstantinou, A.; Katsanevakis, S. Seagrass mapping in Greek territorial waters using Landsat-8 satellite images. *Int. J. Appl. Earth Obs. Geoinf.* **2018**, *67*, 98–113. [CrossRef]
68. Turissa, P.; Bisman, N.; Vincentius, S.; Dony, K.; Hawis, M. Evaluation Methods of Change Detection of Seagrass Beds in the Waters of PajeneKang and Gusung Selayar. *Trends Sci.* **2021**, *18*, 677. [CrossRef]
69. Su, L.; Huang, Y. Seagrass Resource Assessment Using WorldView-2 Imagery in the Redfish Bay, Texas. *J. Mar. Sci. Eng.* **2019**, *7*, 98. [CrossRef]
70. Kovacs, E.M.; Roelfsema, C.; Udy, J.; Baltais, S.; Lyons, M.; Phinn, S. Cloud Processing for Simultaneous Mapping of Seagrass Meadows in Optically Complex and Varied Water. *Remote Sens.* **2022**, *14*, 609. [CrossRef]
71. Manfreda, S.; McCabe, M.F.; Miller, P.E.; Lucas, R.; Pajuelo Madrigal, V.; Mallinis, G.; Ben Dor, E.; Helman, D.; Estes, L.; Ciraolo, G.; et al. On the Use of Unmanned Aerial Systems for Environmental Monitoring. *Remote Sens.* **2018**, *10*, 641. [CrossRef]
72. Johnston, D.W. Unoccupied Aircraft Systems in Marine Science and Conservation. *Annu. Rev. Mar. Sci.* **2019**, *11*, 439–463. [CrossRef]
73. Anderson, K.; Gaston, K.J. Lightweight unmanned aerial vehicles will revolutionize spatial ecology. *Front. Ecol. Environ.* **2013**, *11*, 138–146. [CrossRef]
74. Klemas, V.V. Coastal and Environmental Remote Sensing from Unmanned Aerial Vehicles: An Overview. *J. Coast. Res.* **2015**, *31*, 1260–1267, 1268. [CrossRef]
75. Pell, T.; Li, J.Y.Q.; Joyce, K.E. Demystifying the Differences between Structure-from-Motion Software Packages for Pre-Processing Drone Data. *Drones* **2022**, *6*, 24. [CrossRef]
76. Carpenter, S.; Byfield, V.; Felgate, S.L.; Price, D.M.; Andrade, V.; Cobb, E.; Strong, J.; Lichtschlag, A.; Brittain, H.; Barry, C.; et al. Using Unoccupied Aerial Vehicles (UAVs) to Map Seagrass Cover from Sentinel-2 Imagery. *Remote Sens.* **2022**, *14*, 477. [CrossRef]
77. Duffy, J.P.; Pratt, L.; Anderson, K.; Land, P.E.; Shutler, J.D. Spatial assessment of intertidal seagrass meadows using optical imaging systems and a lightweight drone. *Estuar. Coast. Shelf Sci.* **2018**, *200*, 169–180. [CrossRef]
78. Nahirmick, N.K.; Reshitnyk, L.; Campbell, M.; Hessing-Lewis, M.; Costa, M.; Yakimishyn, J.; Lee, L. Mapping with confidence; delineating seagrass habitats using Unoccupied Aerial Systems (UAS). *Remote Sens. Ecol. Conserv.* **2019**, *5*, 121–135. [CrossRef]
79. Moniruzzaman, M.; Islam, S.; Lavery, P.; Bennamoun, M. Faster R-CNN Based Deep Learning for Seagrass Detection from Underwater Digital Images. In Proceedings of the 2019 Digital Image Computing: Techniques and Applications (DICTA), Perth, Australia, 2–4 December 2019; pp. 1–7.
80. Reus, G.; Möller, T.; Jäger, J.; Schultz, S.T.; Kruschel, C.; Hasenauer, J.; Wolff, V.; Fricke-Neuderth, K. Looking for Seagrass: Deep Learning for Visual Coverage Estimation. In Proceedings of the 2018 OCEANS-MTS/IEEE Kobe Techno-Oceans (OTO), Kobe, Japan, 28–31 May 2018; pp. 1–6.
81. Yamato, C.; Ichikawa, K.; Arai, N.; Tanaka, K.; Nishiyama, T.; Kittiwattanawong, K. Deep neural networks based automated extraction of dugong feeding trails from UAV images in the intertidal seagrass beds. *PLoS ONE* **2021**, *16*, e0255586. [CrossRef]
82. Weidmann, F.; Jäger, J.; Reus, G.; Schultz, S.T.; Kruschel, C.; Wolff, V.; Fricke-Neuderth, K. A Closer Look at Seagrass Meadows: Semantic Segmentation for Visual Coverage Estimation. In Proceedings of the OCEANS 2019, Marseille, France, 17–20 June 2019; pp. 1–6.
83. Rindlisbacher, T.; Chabbey, L. *Guidance on the Determination of Helicopter Emissions*; Federal Office of Civil Aviation FOCA: Bern, Switzerland, 2015; p. 29.
84. Li, K.W.; Sun, C.; Li, N. Distance and Visual Angle of Line-of-Sight of a Small Drone. *Appl. Sci.* **2020**, *10*, 5501. [CrossRef]
85. Cleguer, C.; Kelly, N.; Tyne, J.; Wieser, M.; Peel, D.; Hodgson, A. A Novel Method for Using Small Unoccupied Aerial Vehicles to Survey Wildlife Species and Model Their Density Distribution. *Front. Mar. Sci.* **2021**, *8*, 640338. [CrossRef]
86. Campbell, S.; Rasheed, M.; Thomas, R. *Seagrass habitat of Cairns Harbour and Trinity Inlet: December 2001*; DPI Information Series QI02059; DPI: Cairns, Australia, 2002; p. 25. Available online: <https://bit.ly/3lwyqER> (accessed on 14 March 2022).
87. Oreska, M.P.J.; McGlathery, K.J.; Porter, J.H. Seagrass blue carbon spatial patterns at the meadow-scale. *PLoS ONE* **2017**, *12*, e0176630. [CrossRef]
88. Ricart, A.M.; Pérez, M.; Romero, J. Landscape configuration modulates carbon storage in seagrass sediments. *Estuar. Coast. Shelf Sci.* **2017**, *185*, 69–76. [CrossRef]
89. Ricart, A.M.; York, P.H.; Rasheed, M.A.; Pérez, M.; Romero, J.; Bryant, C.V.; Macreadie, P.I. Variability of sedimentary organic carbon in patchy seagrass landscapes. *Mar. Pollut. Bull.* **2015**, *100*, 476–482. [CrossRef]
90. Carter, A.B.; Collier, C.; Lawrence, E.; Rasheed, M.A.; Robson, B.J.; Coles, R. A spatial analysis of seagrass habitat and community diversity in the Great Barrier Reef World Heritage Area. *Sci. Rep.* **2021**, *11*, 22344. [CrossRef]
91. Rock, B.M.; Daru, B.H. Impediments to Understanding Seagrasses' Response to Global Change. *Front. Mar. Sci.* **2021**, *8*, 608867. [CrossRef]
92. Dalby, O.; Sinha, I.; Unsworth, R.K.F.; McKenzie, L.J.; Jones, B.L.; Cullen-Unsworth, L.C. Citizen Science Driven Big Data Collection Requires Improved and Inclusive Societal Engagement. *Front. Mar. Sci.* **2021**, *8*, 610397. [CrossRef]
93. Jones, B.L.; Unsworth, R.K.F.; McKenzie, L.J.; Yoshida, R.L.; Cullen-Unsworth, L.C. Crowdsourcing conservation: The role of citizen science in securing a future for seagrass. *Mar. Pollut. Bull.* **2018**, *134*, 210–215. [CrossRef] [PubMed]
94. Carter, A.; McKenna, S.; Rasheed, M.; Collier, C.; McKenzie, L.; Pitcher, R.; Coles, R. *Seagrass Mapping Synthesis: A Resource for Coastal Management in the Great Barrier Reef*; NESP TWQ project 3.2.1 and 5.4; Centre for Tropical Water & Aquatic Ecosystem Research (TropWATER), James Cook Univ.: Cairns, Australia, 2020. [CrossRef]

- 
95. Beaman, R.J. *High-Resolution Depth Model for the Great Barrier Reef—30 m*; Geoscience Australia: Canberra, Australia, 2017.
  96. Ronneberger, O.; Fischer, P.; Brox, T. U-Net: Convolutional networks for biomedical image segmentation. In Proceedings of the International Conference on Medical Image Computing and Computer-Assisted Intervention, Munich, Germany, 5–9 October 2015; Springer: Cham, Switzerland, 2015; pp. 234–241.